Functional analysis of a novel cyanobacterial rhodopsin
(シアノバクテリアに由来する新規ロドプシンの機能解析)

Graduate School of Life Science

Hokkaido University

March, 2017

Takatoshi Hasemi

Contents

Abbreviations

- ASR　Anabaena sensory rhodopsin,
- BR　bacteriorhodopsin
- CAPS　*N*-Cyclohexyl-2-aminopropanesulfonic acid
- CCCP　carbonyl cyanide m-chlorophenylhydrazone
- CHES　*N*-Cyclohexyl-2-aminoethanesulfonic acid
- CP　Cytoplasmic
- DDM　n-Dodecyl-ß-D-maltopyranoside
- EC　Extracellular
- *E. coli*　*Escherichia coli*
- FR　*Fulvimarina Pelagi* rhodopsin
- HR　Halorhodopsin
- HsHR　HR from *Halobacterium salinarum*
- ITO　indium tin oxide
- Kd　dissociation constant
- KR2　*Krokinobacter eikastas* rhodopsin 2
- λ_{max}　absorption maximum
- mOD　milli optical density
- MES　2-Morpholinopropanesulfonic acid, monohydrate
- MOPS　3-Morpholinopropanesulfonic acid
- MrHR　HR from *Mastigocladopsis repens*
- NM-R　*Nonlabens marinus* rhodopsin
- NpHR　HR from *Natronomonas pharaonis*
- PC　L-α-phosphatidylcholine
- PR　Proteorhodopsin
- PSB　Protonated Schiff base
- SB　deprotonated Schiff base
- TAPS　N-Tris(hydroxymethyl)methyl-3-aminopropanesulfonic acid
- TES　N-Tris(hydroxymethyl)methyl-3-aminoethanesulfonic acid
- UV　Ultraviolet
- WT　Wild type

Abstract

Microbial rhodopsins are widely distributed in many microorganisms and act as light-driven ion pumps, light sensors and light-gated channels. Ion-pumping rhodopsins are classified into three categories: outward proton (H^+) and sodium (Na^+) pumps and an inward chloride ion (Cl^-) pump. After 1999, advances in genome sequencing techniques led to the discovery of novel rhodopsins in various microbes. Recently, I discovered a novel cyanobacterial rhodopsin group that is distinct from other microbial rhodopsins.

In part 1 of this thesis, I performed functional characterization of the microbial halorhodopsin (MrHR) from the cyanobacterium *Mastigocladopsis repens* and its functional conversion to a H^+ pump. MrHR has the characteristic residues of a Cl^- and H^+ pump. Photo-induced ion transport activity measurement revealed that MrHR acts as inward Cl^--pump. The transportable anions are severely restricted to only Cl^- and Br^-. MrHR bind Cl^- near the protonated Schiff base (PSB) to same extent as that of *Natronomonas pharaonis* halorhodopsin (NpHR). The Cl^- transporting photocycle of MrHR is slower than that of other Cl^- pumps. Through replacement of the 74th threonine with aspartic acid, MrHR was converted to an outward proton pump. The overall photocycle of T74D resembles that of natural H^+ pumps but is prolonged. These results suggest MrHR evolved from a proton pump but not a mature Cl^- pump.

In part 2 of this thesis, I investigated the photoreactions of MrHR and its mutants. Comparison of the photocycle for transportable (Cl^-) and untransportable (I^-) anions revealed that the Cl^- transfer from the extracellular side to the cytoplasmic side occurs during the L-to-N+O transition. However, the sequence of Cl^- release and uptake could not be determined due to the lack of an equilibrium state of the Cl^- concentration. The results of Cl^--induced spectral changes showed that R71, T74, S78, and E182 are

important for Cl^- binding in the dark state. Spectroscopic studies and H^+ transfer reaction measurement suggest that Asp-200 protonates during the unphotolyzed state and deprotonates during L-to-N+O transition. The results of ion-transporting measurement suggest the deprotonation of Asp-200 is necessary to transport Cl^-. In contrast to this protonation during the dark state and deprotonation during the light state, other Cl- pumping rhodopsins maintain the deprotonation of the corresponding aspartic acid in both the dark and light states. This difference might be attributed to the optimization for Cl- pumping.

This study presents the characteristics of a novel chloride-pumping rhodopsin. My findings might be helpful for understanding the functional diversity of microbial rhodopsins and elucidating the mechanism for selecting transportable ions.

General introduction

Organisms from all domains of life possess photoreceptor proteins to utilize light to obtain environmental information and as an energy source. Rhodopsin is a ubiquitous photoreceptor protein[1,2]. Rhodopsin consists of seven transmembrane α-helices that covalently bind retinal, the aldehyde of vitamin A, to the conserved lysine via a Schiff base linkage (Fig. 1). Based on the conserved residues, rhodopsins are classified into two types: animal rhodopsin and microbial rhodopsin. Animal rhodopsins utilize the 11-*cis*/all-*trans* configuration of retinal and act as a signal transducer for vision. Different from animal rhodopsin, microbial rhodopsins utilize the all-*trans*/13-*cis* configuration of retinal and have diverse functions[3,4], including light-driven ion pumping[5], light sensing[6,7] for phototaxis, and the regulation of gene expression[8,9]. Microbial rhodopsins have linear cyclic photochemical reactions called the photocycle (Fig. 2). Upon the light-induced isomerization of retinal, these rhodopsins undergo the respective photocycles in which several intermediates appear and decay sequentially. During the cyclic photoreactions, rhodopsins accomplish the corresponding functions.

In the 1970s, microbial rhodopsins were found in an extremely halophilic archaeon *halobacterium salinarum* (previously referred to as *Halobacterium halobium*). *H. salinarum* contains four rhodopsin genes in its genome. The first discovered microbial rhodopsin was bacteriorhodopsin[10–13] (BR), which acts as an outwardly light-driven proton (H^+) pump. Halorhodopsin[14–16] (HR), an inwardly light-driven chloride pump, was found second. After the discovery of two pumps, two light sensory rhodopsins for phototaxis were identified[17–21]. After 20 years since the discovery of BR, it was considered that microbial rhodopsins were a unique proteins derived from only specific halophilic archaea. However, advances in genome sequencing techniques led to the discovery of

microbial rhodopsins in various microorganism in all domain of life. In 1999, a rhodopsin-like gene was found in the genome of the filament fungus *Neurospore crassa*[22]. In 2000, Beja *et al.* reported proteorhodopsin (PR), an outward H^+ pump found in marine proteobacteria [23]. Later, PR homologues were found in marine eubacteria around the world. In 2002 and 2003, Nagel *et al.* discovered the light-gated proton channel and cation channel rhodopsins (channel rhodopsin-1 and channel rhodopsin-2, respectively) in the green alga *Chlamydomonas reinhardtii*[24,25]. In 2003, Jung *et al.* found a sensory rhodopsin in the cyanobacterium *Anabaena sp.* PCC7120 (ASR)[9]. ASR interacts at the cytoplasmic side with a water-soluble transducer protein[26] and a promotor region of genomic DNA[8], unlike archaeal sensory rhodopsins, which activate membrane-embedded transducer proteins[27]. In 2006, Tsunoda *et al.* reported an outward proton pump in the marine alga *Acetabularia acetabulum*[28]. Inoue *et al.* reported an outward Na^+ pump in the flavobacterium *Krokinobacter eikastus* (KR2)[29] and an inward Cl^- pump from the flavobacterium *Fluvimarina pelagi* (FR)[30]. Recently, Govorunova and coworkers found anion channelrhodopsins from the cryptophyte *Guillardia theta*[31]. Currently, it is considered that microbial rhodopsins are widespread in the microbial world and have diverse functions[32–34]. In particular, ion-pumping rhodopsins are abundant and widely distributed due to being the most convenient for light energy utilization.

Ion-pumping rhodopsins are categorized into three types[5]; outward proton and sodium pumps and an inward chloride pump. Despite their functional diversity, their protein architectures are essentially same. Thus, these rhodopsins appear to share a common transport machinery where the transportable ions are determined by the essential amino acid residues at appropriate positions. This scenario was partially demonstrated in 1995, when the H^+-pumping rhodopsin BR was converted to an inward Cl^- pump by the single

amino acid replacement of Asp-85 with threonine based on the amino acid in the Cl^- pump HR[35]. In contrast, the reverse conversion, that is, from a Cl^- pump to a H^+ pump, has not been achieved[35–37], even after 10 mutations of HR[37].

In this thesis, I investigated a novel rhodopsin derived from the terrestrial cyanobacterium *Mastigocladosis repens*. I called this protein MrHR. Because MrHR has the characteristic residues of both Cl^- and H^+ pumps, MrHR is good research subject for elucidating the relationship between H^+ pumps and Cl^- pumps. In part 1 of this thesis, I characterized the Cl^--pumping activity of MrHR and its functional conversion to a H^+ pump. In part 2 of this thesis, I performed a photochemical analysis of MrHR and its mutants to investigate the details of the Cl^--transporting photocycle.

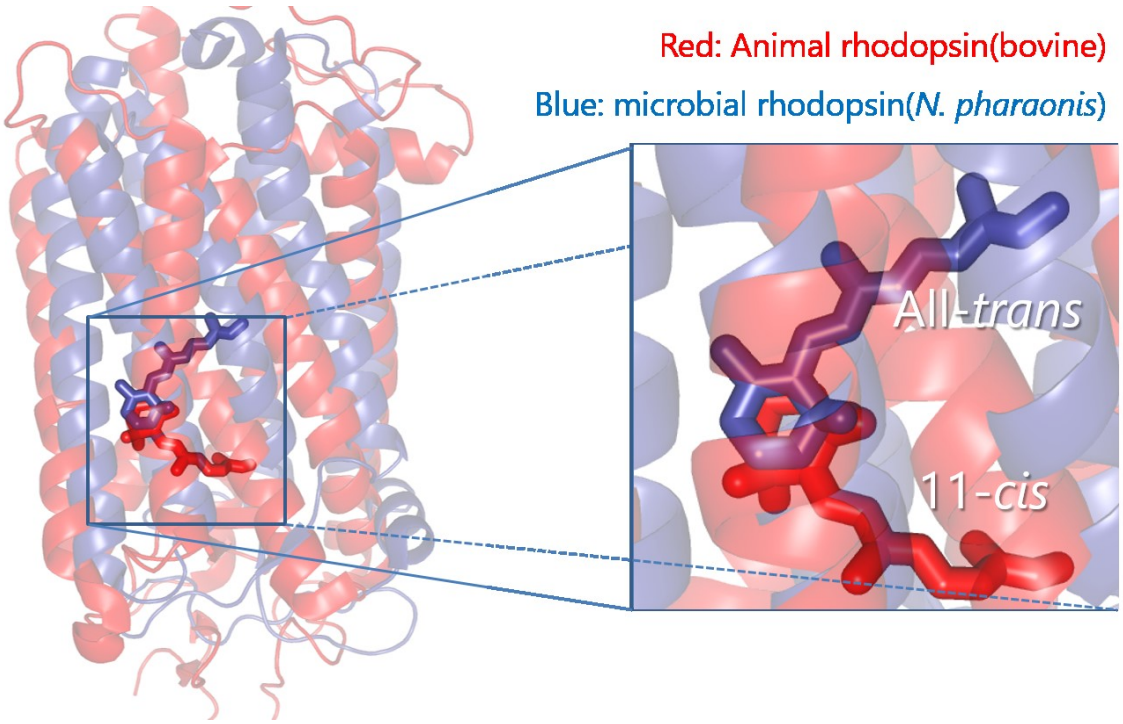

FIGURE 1. Comparison of the structures of animal rhodopsin and microbial rhodopsin. The structure of halorhodopsin from the halophilic archaea *Natronomonas pharaonis* (PDB code: 3A7K) is shown in red. The structure of bovine rhodopsin (PDB code: 1U19) is shown in blue. The region around retinal is magnified.

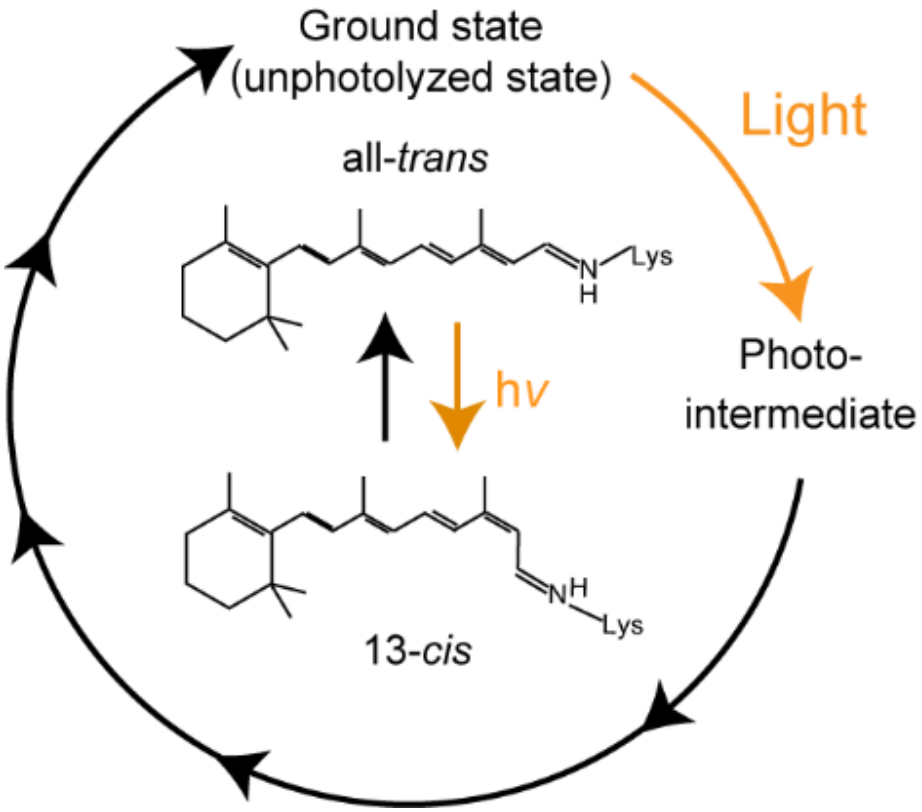

FIGURE 2. Simplified model of the photocycle.

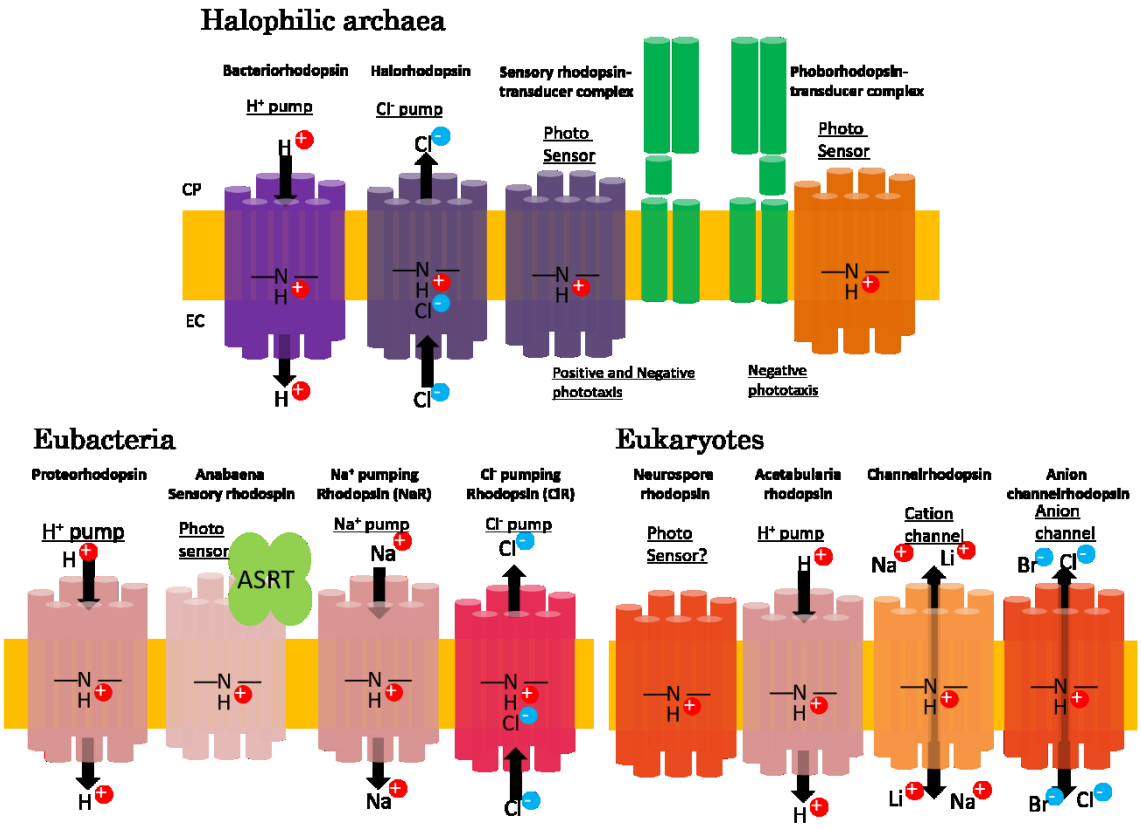

FIGURE 3. Functional diversity of microbial rhodopsins

Part I

Discovery of a Cyanobacterial Chloride-pumping Rhodopsin and Its Conversion into a Proton Pump

Ⅰ-1 Abstract

Light-driven ion-pumping rhodopsins are widely distributed in microorganisms and are now classified into the categories of outward H^+ and Na^+ pumps and an inward Cl^- pump. These different types share a common protein architecture and utilize the photoisomerization of the same chromophore, retinal, to evoke photoreactions. Despite these similarities, successful pump-to-pump conversion had been confined to only the H^+ pump bacteriorhodopsin, which was converted to a Cl^- pump in 1995 by a single amino acid replacement. In this study, we report the first success of the reverse conversion, from a Cl^- pump to a H^+ pump. A novel microbial rhodopsin (MrHR) from the cyanobacterium *Mastigocladopsis repens* functions as a Cl^- pump and belongs to a cluster that is far distant from the known Cl^- pumps. With a single amino acid replacement, MrHR is converted to a H^+ pump in which dissociable residues function almost completely in the H^+ relay reactions. MrHR most likely evolved from a H^+ pump, but it has not yet been highly optimized into a mature Cl^- pump.

Ⅰ-2 Introduction

Rhodopsins are ubiquitous membrane proteins that enable the cellular utilization of light as an information and energy source. According to their conserved residues, they are classified into two groups (1,2). One is animal rhodopsin, represented by visual pigments in the eyes. The other is microbial rhodopsin, which shows divergent functions in unicellular microorganisms, such as light-driven ion pumps and light sensors for phototaxis and the regulation of gene expression. Different from animal rhodopsins, the microbial sensors represent a minority of the microbial rhodopsins. However, microbial sensors have individualities in their signal-transduction modes, which include interactions with other membrane proteins, interactions with cytoplasmic components, and light-gated ion channel activity.

Microbial rhodopsins were originally discovered in highly halophilic archaea in the early 1970's – 1980's (3). Since 1999, their homologues have begun to be identified in various microorganisms inhabiting a broad range of environments (4-6). It is now clear that in the microbial world, ion-pumping rhodopsins are abundant and widely distributed. In microorganisms, these ion pumps are probably the most convenient system for light energy utilization. The first and second ion pumps to be discovered were bacteriorhodopsin (BR) (7) and halorhodopsin (HR) (8) from halophilic archaea, which are an outward H^+ pump and an inward Cl^- pump, respectively. In 2000, an outward H^+ pump named proteorhodopsin (PR) was discovered in a marine proteobacterium (9). Later, the PR homologues were identified in eubacteria living in the oceans worldwide (10). Recently, two groups of ion pumps, the outward Na^+ pump (NaR) and inward Cl^- pump (ClR), were also discovered in eubacteria (11,12). Their representatives are *Krokinobacter eikastus* rhodopsin 2 (KR2) (13) and *Fulvimarina pelagi* rhodopsin (FR)

(14), respectively. The phylogenetic position of these ion pumps is shown in Fig 1A. In contrast to their functional diversity, these ion pumps have essentially the same structural folds composed of seven helices and the chromophore retinal, which binds to a conserved lysine residue *via* a protonated Schiff base (PSB; deprotonated Schiff base is abbreviated as SB). In the dark, most ion-pumping rhodopsins dominantly contain retinal with the all-*trans* configuration, while some minorities such as BR and HR from archaeon *Halobacterium salinarum* (HsHR) can also accommodate 13-*cis* retinal (2). Regardless of this difference in the dark states, only the photoisomerization from all-*trans* to 13-*cis* can trigger the conformational changes for respective ion pumping functions. Thus, ion-pumping rhodopsins appear to share a common transport machinery, where the transportable ions are probably determined by essential residues at appropriate positions. This scenario was partially demonstrated in 1995, when the H^+ pump BR was converted to an inward Cl^- pump by the single amino acid replacement of Asp85 with Thr, the corresponding amino acid in HR (15). However, the success of pump-to-pump conversion was confined to this BR case. The reverse conversion, that is, from a Cl^- pump to a H^+ pump, has not been achieved (16-18) even after ten mutations of HR (18). Here, we report a new class composed of an inward Cl^- pump and its conversion to an outward H^+ pump. Functional characterization was performed with a microbial rhodopsin from the cyanobacterium *Mastigocladopsis repens*, which was isolated from soil at Punta de la Mora, Tarragona in Spain. This microbial rhodopsin is designated as *M. repens* HR (MrHR) due to its similarities with HR. By a single amino acid replacement, MrHR begins to pump H^+ outwardly. Thus, this is the first successful conversion from an inward Cl^- pump to an outward H^+ pump.

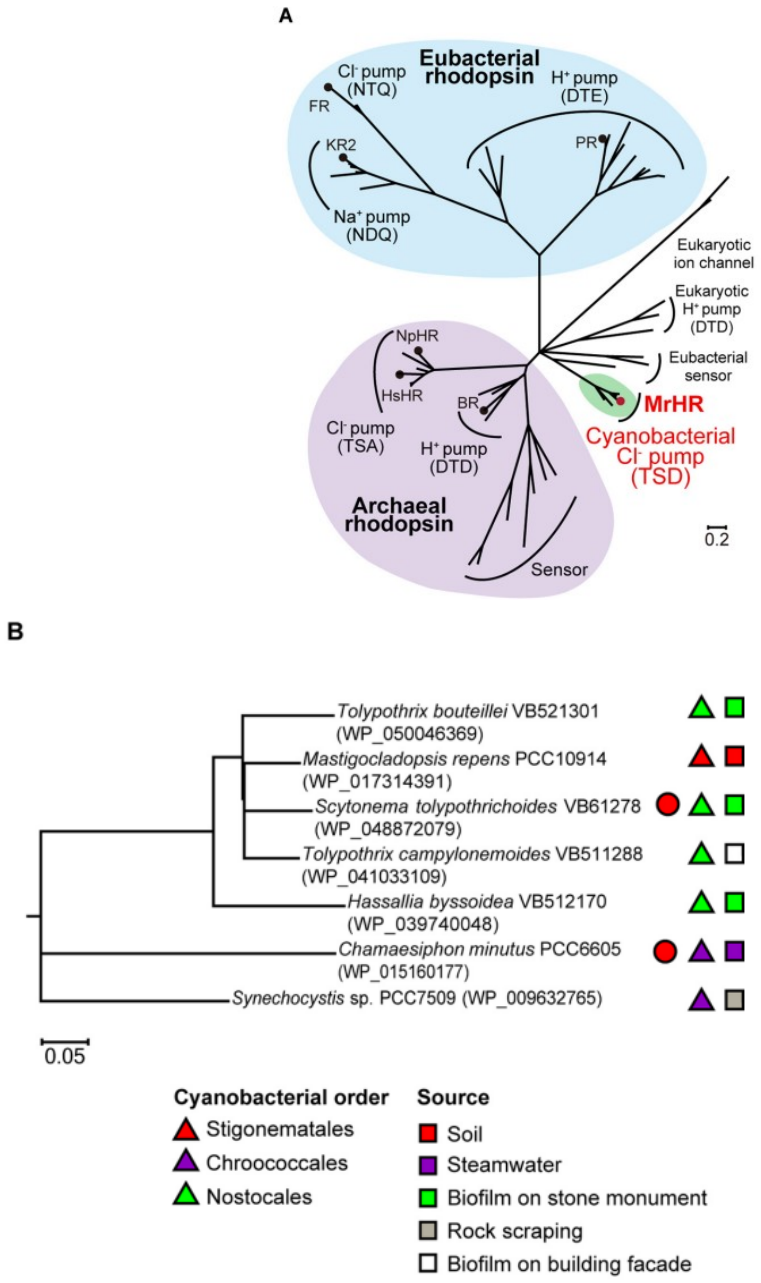

FIGURE 1. Phylogenetic relationships of microbial rhodopsins. A, unrooted tree of microbial rhodopsins showing their functional diversity. The representative ion pumps are shown with the circles. Green is the clade consisting of the MrHR homologues. NpHR, HR from *Natronomonas pharaonis*. B, phylogenetic tree of the MrHR homologues. Their NCBI accession IDs are indicated in the parentheses. The strains labeled with closed circles also contain the Anabaena sensory rhodopsin gene. Other symbols indicate the cyanobacteria orders and the sources of the host strains. In both trees, nodes with 50% bootstrap percentages are collapsed.

Ⅰ-3 Materials and Methods

Phylogenetic Analysis

The 57 amino acid sequences were aligned using MUSCLE. All sequence data were obtained from the NCBI database. The phylogenetic tree was constructed by using the maximum likelihood method, with bootstrap percentages based on 1,000 replications. Initial trees for the heuristic search were obtained by applying the neighbor-joining method (19). Evolutionary distances were calculated with the JTT matrix-based method (20). The branch lengths denote the number of amino acid substitutions. All analyses were performed using MEGA6.

Gene Preparation

Escherichia coli strain DH5α was used for DNA manipulation. An MrHR gene (NCBI accession ID: WP_017314391) with codons optimized for *E. coli* expression was chemically synthesized (Funakoshi, Japan) and inserted into the NdeI/XhoI site of the pET-21c(+) vector (Merck Japan, Tokyo, Japan). This plasmid results in MrHR with additional amino acids in the C-terminus (-LEHHHHHH). The T74D mutation was introduced using the QuikChange Site-Directed Mutagenesis Kit (Stratagene, La Jolla, CA). The DNA sequences were confirmed by a standard method using an automated DNA sequencer (model 3100, Applied Biosystems, Foster City, CA).

Protein Expression and Purification

MrHR and the T74D mutant were expressed and purified from *E. coli* BL21(DE3) cells. The procedures were essentially the same as those previously described (21). The cells were grown at 37 ºC in 2×YT medium supplemented with 50 μg/mL ampicillin. At the late exponential growth phase, the expression was induced by the addition of 1 mM

isopropyl-ß-D-thiogalactpyranoside in the presence of 10 µM all-*trans* retinal. After 3 h of induction, pink-colored cells were harvested by centrifugation (6400 × g, 8 min at 4 °C) and washed once with buffer (50 mM Tris-HCl, pH 8.0) containing 5 mM $MgCl_2$. Then, the cells were broken with a French press (Ohtake, Tokyo, Japan) (100 MPa × 4 times). After removing the undisrupted cells by centrifugation (5600 × g, 10 min at 4 °C), the supernatant was ultracentrifuged (178,000 × g, 90 min at 4 °C). The collected cell membrane fraction was suspended with the same buffer containing 300 mM NaCl and 5 mM imidazole and was then solubilized with 1.5% n-dodecyl ß-D-maltopyranoside (DDM) (Dojindo Lab, Kumamoto, Japan) at 4 °C overnight. After removal of the insoluble fraction by ultracentrifugation (178,000 × g, 60 min at 4 °C), the solubilized MrHR proteins were subjected to Ni-NTA agarose (Qiagen, Hilden, Germany). The unbound proteins were removed by washing the column with 10 column volumes of wash buffer (50 mM sodium phosphate, pH 7.5) containing 400 mM NaCl, 50 mM imidazole and 0.05% DDM. The bound protein was eluted with buffer (50 mM Tris-HCl, pH 7.0) containing 300 mM NaCl, 500 mM imidazole and 0.1% DDM. The yield of MrHR was 15 mg from 1 L culture. The concentration was determined from the absorbance at 537 nm under an assumed extinction coefficient of 40,000 $M^{-1}cm^{-1}$. The purified samples were replaced with an appropriate buffer solution by passage over Sephadex G-25 in a PD-10 column (Amersham Bioscience, Uppsala, Sweden).

Ion Pump Activity Measurements

The MrHR activity was measured in *E. coli* suspensions using a conventional pH electrode method (22), which detects the pH changes by the pump activity of H^+ itself or passive H^+ transfer in response to the membrane potential created by the pump activity

for another ion. The *E. coli* suspensions were prepared as follows. The cells expressing MrHR were harvested at 3,600 g for 5 min at 4 °C and washed twice with an unbuffered solution containing 200 mM salt (NaCl, Choline-Cl, NaBr, NaI or $NaNO_3$). They were resuspended in the same salt solution and gently shaken overnight at 4 °C in the presence of 10 µM carbonyl cyanide m-chlorophenylhydrazone (CCCP). Then, the cells were washed twice with the same salt solution without CCCP and finally suspended at an A_{660} of 0.5. This cell density was approximately 5% of the corresponding value for the original culture medium. As deduced from the purification yield, the original culture medium contains at least 15 µg/mL MrHR. Thus, the cell suspensions for the activity measurements contain at least 0.75 µg/mL of MrHR. For the activation of MrHR, 530 ± 17.5 nm green LED (LXHL-LM5C, Philips Lumileds Lighting Co., San Jose, CA) was used.

HPLC Analysis

The retinal configurations of MrHR were examined in both of the dark/light-adapted states. For dark adaptation, the MrHR samples were kept in the dark for 1 week in 10 mM MOPS, pH 6.5, containing 100 mM NaCl and 0.05% DDM. For light adaptation, the samples were irradiated for 2 min by green LED light as described above. MrHR undergoes a prolonged photocycle as described below. To avoid the contamination of retinal in the photolyzed state, the retinal oxime extraction was carried out after 1 min incubation in the dark. The extraction and the following HPLC analysis was performed as previously described (22).

Absorption Spectra Measurements and Flash Photolysis

UV-visible spectra of MrHR samples were measured with a UV-1800 spectrometer

(Shimadzu, Kyoto, Japan). Flash-induced absorbance changes were obtained in the 5 μs to 10 s time range on a single wavelength kinetic system. For the photoexcitation, the second harmonic (7 ns, 532 nm) of a Q-switched Nd:YAG laser (Surelite I-10, Continuum, Santa Clara, CA) was used. The details have been previously described (21). To improve the S/N ratio, 30 laser pulses were used at each measurement wavelength. All measurements were performed at 25 ºC.

Ⅰ-4 Results and Discussion

Phylogenetic analysis

Mastigocladopsis repens, isolated from the surface of soft powdery calcareous soil, is a blue-green alga belonging to the cyanobacterial order Stigonematales and was morphologically characterized according to the filaments it forms, which have many branches (23). In 2013, the existence of a gene encoding a microbial rhodopsin was revealed by whole genome sequencing of *M. repens* (24). We named this microbial rhodopsin "*M. repens* halorhodopsin (MrHR)" after its photochemical properties, described below. At present, six other homologues of MrHR are found in the NCBI database. Figure 1A shows the phylogenetic tree of microbial rhodopsins, which revealed that MrHR homologues constitute a new clade that is distinct from the known microbial rhodopsins. The six homologues are also encoded in cyanobacteria and share 63-89% amino acid identities with MrHR. Meanwhile, the host strains belong to different cyanobacterial orders (Chroococcales and Nostocales) from *M. repens*, reflecting morphological differences. The phylogenetic relationships of MrHR homologues are shown in Fig 1B together with the names, orders and sources of their host strains. In addition to *M. repens*, all other genomes were sequenced (24-28). Cyanobacteria are a genetically diverse group and are widespread in fresh water, marine, terrestrial and extreme environments such as hot springs and salt lakes. However, out of the seven strains of MrHR homologues, six were isolated from terrestrial environments, such as soil and rock scrapings, and biofilms on stone monuments and building facades (Fig 1B) (23,29,30). Correspondingly, the desiccation resistance was experimentally confirmed for several strains (31). Two strains also contain the gene for *Anabaena* sensory rhodopsin (ASR), a putative sensor for chromatic adaptation that was originally discovered in the

cyanobacterium *Anabaena* sp. PCC7120 (32). The other five strains do not contain other microbial rhodopsin genes.

Microbial rhodopsins are largely categorized into ion pumps and sensors. All ion pumps are solely encoded in their respective operons in the genomes, whereas all sensors are encoded to be adjacent to the genes encoding the cognate transducers within the same operons. For MrHR homologues, their genes are solely encoded, implying that they function as ion pumps.

Comparison of the important residues among ion-pumps.

Previous studies on ion pumps (12,13) have indicated that three amino acids are responsible for determining the transportable ions (Fig 2A and B). For H^+ pumps, a H^+ from PSB is translocated during the photoreaction. This H^+ is initially transferred to D85 in BR (D97 in PR), and SB subsequently accepts a H^+ from D96 in BR (E108 in PR) (Fig 2A). These residues are often referred to as the H^+ acceptor and donor, respectively. For Cl^- pumps, the acceptor is replaced with a 'T' in HR and 'N' in FR (Fig 2B), which enables the binding of substrate Cl^- as the counter ion of the PSB. Furthermore, for HR and KR2, another residue corresponding to T89 in BR is known to play a crucial role (13,21): These residues are 'S' in HR and 'D' in KR2, respectively (Fig 2B). Thus, three residues (D85, T89, and D96 in BR) are now designated as the "motif": These are DTD and DTE for BR and PR, TSA for HR, and NTQ and NDQ for FR and KR2 (Fig 2B). For MrHR, the motif is TSD (Fig 2A and B), which is close to TSA in HR. This implies that MrHR may pump Cl^- inwardly, despite a low amino acid identity of 22% for HR and 12% for FR. The identities for the H^+ pumps are also low: 29% for BR and 17% for PR. However, the donor in the H^+ pumps is conserved as 'D' in MrHR, similar to BR(D) or PR(E). Furthermore, MrHR conserves E194 and E204 in BR, which consists of the H^+ releasing

complex to the extracellular medium (Fig 2B). Thus, MrHR conserves the residues that are characteristic of both the Cl^- pump (HR) and the H^+ pump (BR and PR).

A

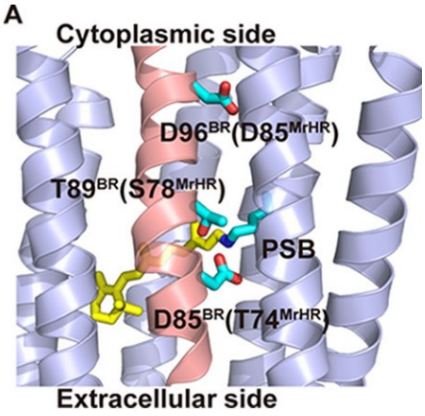

B

No. in BR		82	**85**	**89**	**96**	194	204	212	216
No. in MrHR		71	**74**	**78**	**85**	182	192	200	204
H^+ pump	**BR**	R	**D**	**T**	**D**	E	E	D	K
	PR	R	**D**	**T**	**E**	L	L	D	K
Na^+ pump	**KR2**	R	**N**	**D**	**Q**	L	R	D	K
Cl^- pump	**FR**	R	**N**	**T**	**Q**	L	R	D	K
	NpHR	R	**T**	**S**	**A**	E	T	D	K
	MrHR	R	**T**	**S**	**D**	E	E	D	K

FIGURE 2. A, positions of three amino acid residues consisting of the motif. X-ray crystal structure of BR (PDB code 1C3W) is shown from a view parallel to the membrane. The central part is magnified and the helix C is shown in pink. Three motif residues, Asp-85, Thr-89, and Asp-96, are shown in sticks together with the retinal bound to Lys-216 via PSB. The corresponding residues in MrHR, Thr-74, Ser-78, and Asp-85 are indicated in the parentheses. B, comparison of the important residues, especially the motifs among the ion pumps. NpHR, HR from *Natronomonas pharaonis*.

Ion-transporting activity of wild type MrHR

In this study, I expressed MrHR in the cell membrane of *Escherichia coli* and investigated the ion-pumping activity using the light-induced pH changes of the cell suspensions (Fig 3). In a NaCl solution, light-induced alkalization was observed. This pH change was not abolished by the addition of the protonophore CCCP, which eliminates the electrochemical gradient of the proton (33). This means that the alkalization was not caused by the active proton transport but was caused by the passive proton influx in response to the interior negative membrane potential, which should be created by outward Na^+ or inward Cl^- translocation. In Choline-Cl, alkalization was also observed. Because choline is a large organic cation, microbial rhodopsin cannot transport it. This indicates that MrHR functions as a light-driven inward Cl^- pump. The pump activity decreased in NaBr and disappeared in NaI and $NaNO_3$. Thus, MrHR does not pump Na^+ but does pump smaller anions. The transportable anions are severely restricted to only Cl^- and Br^-, different from HR and FR, which can even transport NO_3^- (14,33).

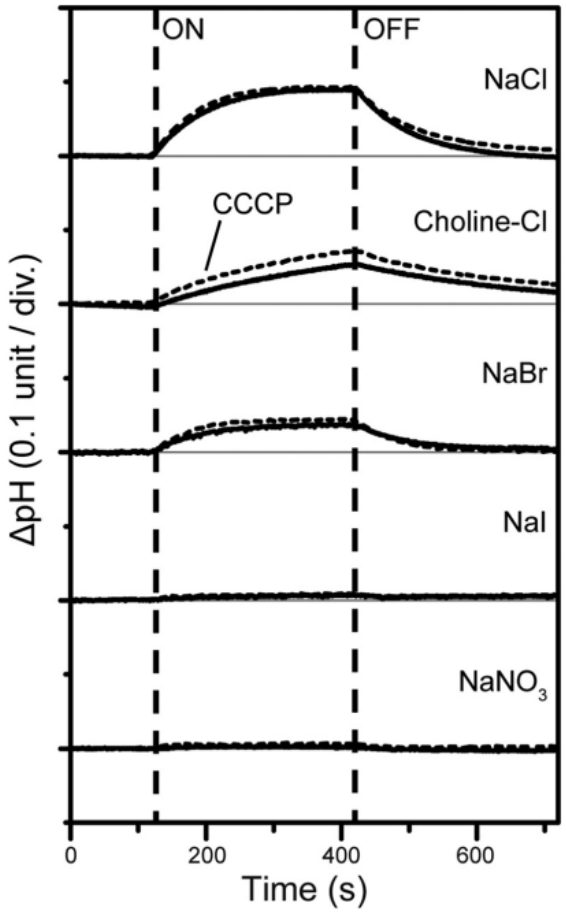

FIGURE 3. Light-induced pH changes by MrHR expressed in E. coli cells. The cells were suspended in a 200 mM salt solution without (solid lines) and with (broken lines) 10 μM CCCP.div.,division.

The retinal Isomer Composition of Wild-type MrHR

The retinal isomer composition of MrHR was examined by HPLC analysis (Fig. 4). As described above, BR and HsHR in the dark states can accommodate both all-*trans* and 13-*cis* retinals and show so-called "light-dark adaptation" (2). In their light-adapted states after continuous illumination the unphotolysed states predominantly contain all-*trans* retinal. Upon dark adaptation, their 13-*cis* contents increased ~50%. For MrHR (Fig. 4), the isomer composition did not depend upon the dark/light adaptation and was predominantly all-*trans*, similar to most ion-pumping rhodopsins. Thus, the all-trans retinal is responsible for the ion-pumping function of MrHR.

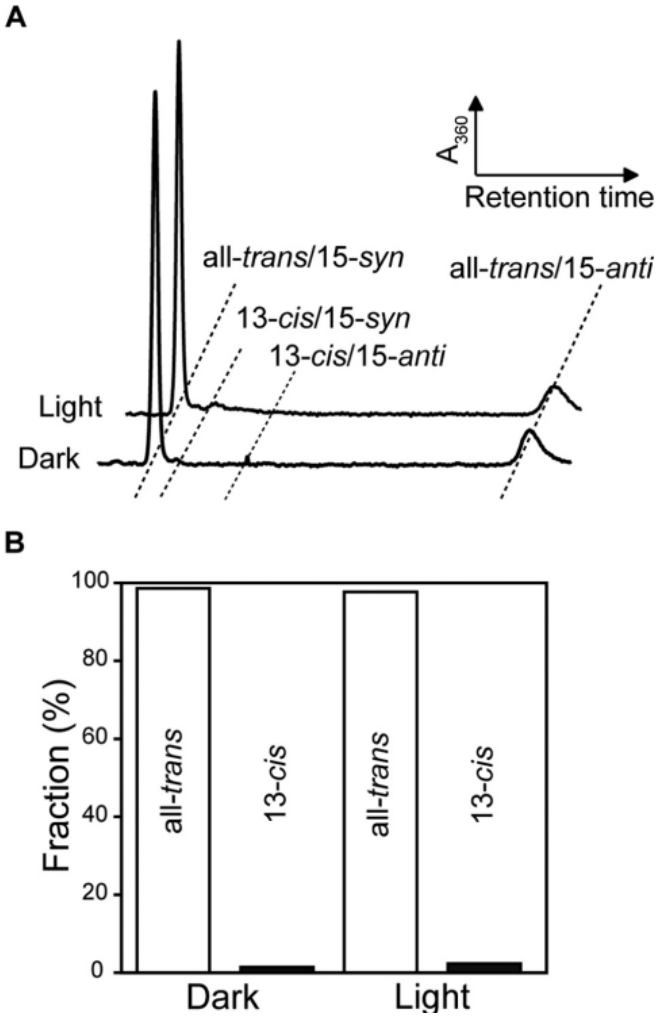

FIGURE4.Retinal isomer compositions of MrHR in dark and light-adapted states. A, HPLC chromatographs of the retinal isomer extracted from MrHR. B, ratios of all-trans and 13-cis retinals determined from the peak areas. The all-trans configuration was dominant (~98%), independent of the dark- and light-adapted states.

Spectroscopic characterization of WT-MrHR

Anion binding near the PSB was monitored by the color change of retinal using purified MrHR (Fig 5A). For other Cl^- pumps, Cl^- binding causes a blueshift (14,34), except for HsHR (22). In contrast, a large redshift occurs for MrHR by its binding of Cl^-, suggesting the differences in the Cl^- binding site from other Cl^- pumps. Similar redshifts were also observed for Br^- and even for I^- and NO_3^-. The dissociation constants (K_d) were determined from the absorbance changes at 550 nm (Fig 5B), and the results are summarized in Table 1. The K_d values are close to those of HR, except for NO_3^- (171 mM): HR binds NO_3^- more strongly (K_d ~ 16 mM) (35), whereas FR binds these ions more weakly (K_d = 40 – 130 mM) (14). These results indicate that MrHR can bind I^- and NO_3^- but cannot transport them. These larger ions may be impossible to move toward a cytoplasmic half channel over the PSB region. Compared with HR and FR, the ion translocation pathway might be narrow and act as an ion-selective filter.

We also characterized the photocycle of MrHR by a flash photolysis method. Time-dependent absorbance changes at selected wavelengths are shown in Fig 5C, which indicates that the photocycle of MrHR is very slow due to the prolonged decay of the last intermediate (540 nm). Ion-pumping rhodopsins transport one ion during a single turnover of photocycle and generally undergo fast photocycles (< 100 ms), which enable the generation of a large transmembrane electrochemical potential under constant illumination. On the other hand, similar to HR and FR, no absorbance change at 400 nm was observed throughout the photocycle (14,34,36), indicating that there was no formation of a M intermediate, which is expected in H^+ pumps and reflects the deprotonation of PSB. The observed intermediates and the order of their appearance resembles those of HR. These intermediates are (the estimated λ_{max} are indicated in the

parentheses): K (540 nm) → L (460 nm) → N (460 nm) + O (620 nm) → MrHR' (540 nm). "N (460 nm) + O (620 nm)" means that the quasi-equilibrium between N and O appeared in the time period between 3 – 50 ms. A similar equilibrium was also observed for HR (34,37). The last intermediate MrHR' corresponds to HR' in HR but has a substantially longer lifetime (~ 6 s).

The slow photocycle of MrHR might reflect some differences in the physiological role from other Cl^--pumping rhodopsins. Although the details are not fully resolved, the Cl^- pumps are believed to play roles in light-driven ATP production and/or maintaining the cellular osmotic balance during the volume increase of the growing cell (38-41). All host strains of MrHR homologues contain a photosynthetic apparatus. Thus, the slow photocycle of MrHR seems to contribute little to cellular ATP production under illumination. Instead, MrHR might relate to a regulation of osmotic pressure. Unlike aquatic cells harboring other Cl^- pumps, most host strains of MrHR homologues inhabit terrestrial and non-aquatic environments, where the cells are occasionally exposed to draught stress. Thus, the cells might utilize MrHR homologues to survive in the non-aquatic habitats. Under desiccated conditions, the internal salt concentration should be increased to preserve the intracellular water content. Due to the interior negative membrane potential, cations could be passively transported inside. However, anions need an active transport system, such as MrHR. Thus, a simple scenario might be that MrHR elevates the intracellular osmotic pressure, which in turn preserves the intracellular water content under drought conditions. For further discussion, we must await future investigations.

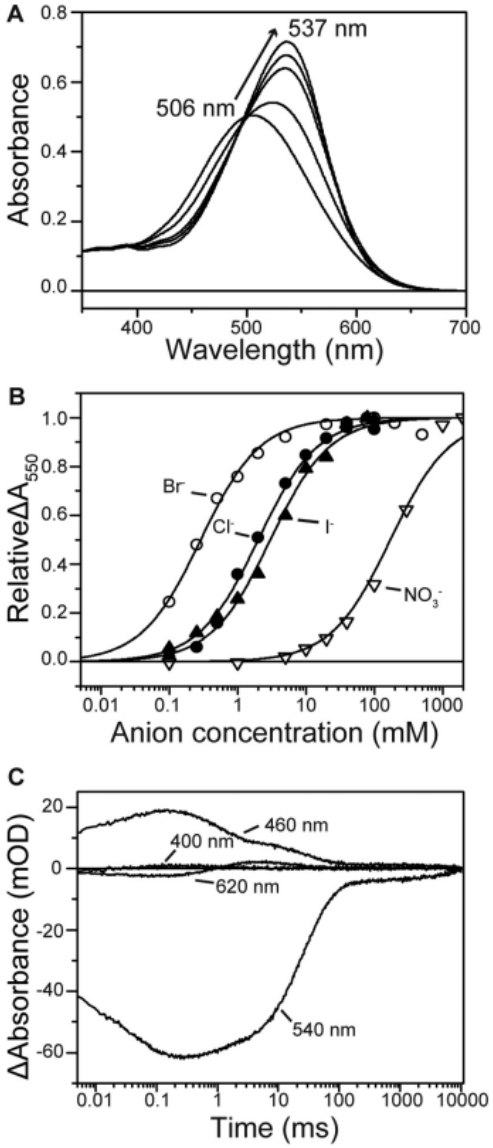

FIGURE 5. Spectroscopic characterization of MrHR. A, absorption spectral red shift by the Cl- binding to the unphotolysed state. The medium (pH 6.5) contained 33 mM Na_2SO_4, 0.05% DDM, and NaCl (0-100 mM). B, titration with various anions, which were added by sodium salts. The relative absorbance changes at 550 nm are plotted. C, flash-induced absorbance changes at selected wavelengths. The medium (pH 6.5) contained 0.05% DDM and 100 mM NaCl. mOD, milli-optical density.

Dissociation constants (K_d), absorption maxima (λ_{max}) and their shifts ($\Delta\lambda_{max}$) by the anion bindings

[a]K_ds were determined by fitting analyses using Hill equation with n = 1. The best-fit curves are shown in Fig 5B.

[b]λ_{max}s were the determined values at the following anion concentrations: Cl^-, 0.5 M; Br^-, 0.5 M; I^-, 0.5 M; NO_3^-, 2 M. At these concentrations, the λ_{max} shifts were almost saturated.

[c]$\Delta\lambda_{max}$s denote the λ_{max} shifts from the anion-free state (506 nm).

Anions	K_d (mM)[a]	λ_{max} (nm)[b]	$\Delta\lambda_{max}$ (nm)[c]
Cl^-	1.99 ± 0.11	537	31
Br^-	0.28 ± 0.08	538	32
I^-	2.99 ± 0.21	535	29
NO_3^-	171 ± 20.6	532	26

Functional conversion into outward H^+ pump

MrHR conserves the H^+ donor residue in the H^+ pump, which is an essential residue in the H^+ pump. Thus, I attempted the conversion of the MrHR to a H^+ pump; a mutant T74D was made in which the Asp residue was introduced as a possible proton acceptor. The λ_{max} of T74D is located at 522 nm (Fig 6A) and did not change upon the addition of Cl^-. This indicates that there is no chloride binding near the PSB. The HPLC analyses showed that the retinal isomer composition is predominantly all-*trans* (> 95%) in both dark and light-adapted states, similar to wild-type MrHR. Next, we examined the ion-pumping activity using the pH change of the *E. coli* suspension. The results are shown in Fig 6B, which indicates the opposite pH change to the wild-type MrHR. Even in the NaCl solution, light-induced acidification was observed, showing proton extrusion. This pH change was decreased by the addition of CCCP, indicating that T74D actively pumps protons outward. Thus, a successful conversion from a Cl^- pump to a H^+ pump was effected by the single amino acid replacement. Corresponding to this conversion, T74D undergoes a totally different photocycle from that of wild-type MrHR (Fig 6C). Specifically, the M-formation (400 nm) was observed, indicating that the introduced Asp residue acts as a H^+ acceptor from PSB. For HR, a T-to-D mutation was never observed to induce M-formation (16-18). For natural H^+ pumps in the dark, SB is protonated while the acceptor is deprotonated because the SB has a larger pKa than the acceptor. M-formation requires the inversion of the pKa values: The pKa of the acceptor must become larger than that of SB. T74D accomplishes these pKa changes. Following M decay, two intermediates appear sequentially, corresponding to N (470 nm) and O (590 nm) in BR. For H^+ pumps, the donor facilitates both M-N and N-O transitions because the M-N transition reflects proton movement from the donor to SB, and the subsequent N-O

transition reflects proton uptake from the cytoplasmic medium by the donor. Thus, the donor-lacking mutants of H^+ pumps undergo substantially slower transitions after M formation (42,43). Interestingly, both transitions in T74D are fast compared with natural H^+ pumps, indicating that the donor functions very well. Moreover, M, N and O appear sequentially without quasi-equilibrium. This reflects the strict "accessibility switch" of the donor, which communicates with SB during the M-N transition; then, the accessibility switches to the cytoplasmic medium to facilitate the N-O transition. In a H^+ pump, this switch contributes to the one-way (irreversible) H^+ transport (42,43). These facts indicate that T74D contains the structural factors as well as the essential residues for an effective H^+ pump. The overall photocycle of T74D resembles that of natural H^+ pumps but is prolonged due to the last intermediate (520 nm), which resembles MrHR in the wild-type photocycle. A similar intermediate was also observed in PR (44), but MrHR in T74D had a substantially long lifetime (~3 s). Another difference from a natural H^+ pump is the formation of an unknown intermediate (hereafter called X) at ~440 nm. X is formed almost simultaneously with the M-decay, but it decays independently of N and O. Thus, X probably forms from M by a branching process. SB reprotonates during the M-decay. For the M-N transition, the donor provides this proton. For the M-X transition, the proton is probably provided through another pathway, implying no contribution of X to the H^+ pumping activity. In natural H^+ pumps, the antecedent deprotonation of SB triggers the accessibility switching of SB from the acceptor to donor, which enables the exclusive H^+ transfer from the donor to SB (42, 43). In T74D, this switching might not be stringently controlled.

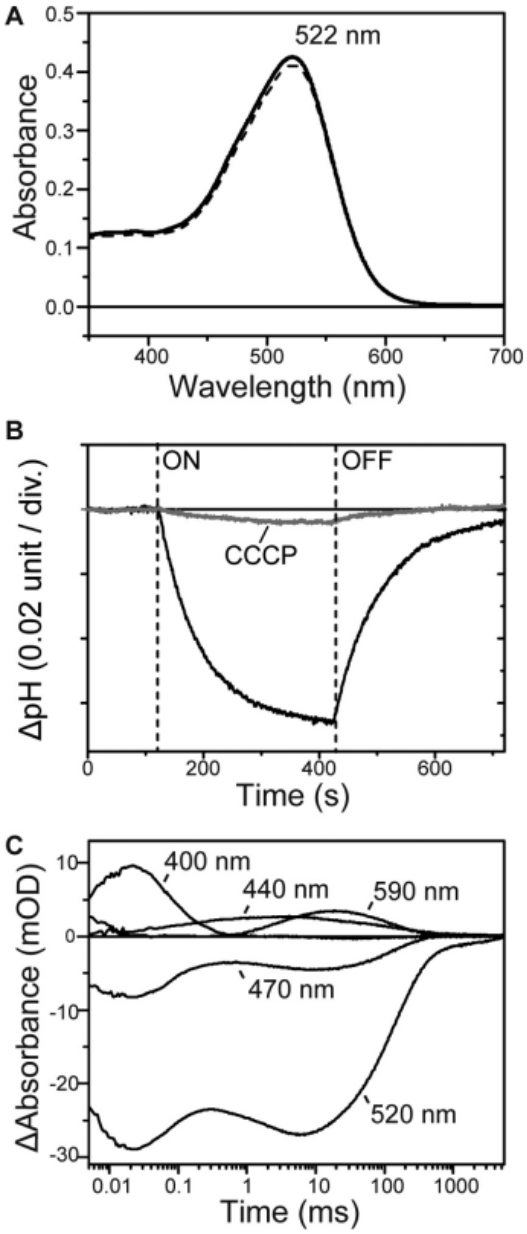

FIGURE 6. Characterizations of T74D MrHR. A, absorption spectra in the unphotolysed state. The medium (pH 6.5) contained 0.05% DDM and 33 mM Na2SO4 (solid line) or 500 mM NaCl (broken line). B, light-induced pH changes by T74D expressed in *E. coli* cells in 200 mM NaCl without and with 10 μM CCCP. div., division. C, flash-induced absorbance changes at selected wavelengths. The medium (pH 6.0) contained 0.05% DDM and 100 mM NaCl. *mOD*, milli-optical density.

Ⅰ-5 Conclusion

MrHR functions as an inward Cl^- pump but undergoes a prolonged photocycle. The donor residue is not essential for Cl^--pumping activity, which was confirmed by the alanine replacement mutant (data not shown). In contrast, in T74D, both the introduced acceptor and the conserved donor function are comparable with those in natural H^+ pumps, which suggests that MrHR evolved from a H^+ pump, but the residues and the structure have not been optimized into a mature Cl^- pump. The mutant T74D has reduced H^+ pumping activity as compared to natural H^+ pumps because of the slow decay of the last intermediate and the formation of the X intermediate. These weaknesses are probably related to the lost mechanisms, which are MrHR functions as an inward Cl^- pump but undergoes a prolonged photocycle. The donor residue is not essential for Cl^--pumping activity, which was confirmed by the alanine replacement mutant (data not shown). In contrast, in T74D, both the introduced acceptor and the conserved donor function are comparable with those in natural H^+ pumps, which suggests that MrHR evolved from a H^+ pump, but the residues and the structure have not been optimized into a mature Cl^- pump. The mutant T74D has reduced H^+ pumping activity as compared to natural H^+ pumps because of the slow decay of the last intermediate and the formation of the X intermediate. These weaknesses are probably related to the lost mechanisms, which are and H^+ pumps might provide insight into how sophisticated Cl^- pumps evolved from H^+ pumps.

Ⅰ-6 References

1. Heberle, J., Deupi, X., and Schertler, G. (2014) Retinal proteins - you can teach an old dog new tricks. *Biochim. Biophys. Acta* **1837**, 531-532
2. Ernst, O. P., Lodowski, D. T., Elstner, M., Hegemann, P., Brown, L. S., and Kandori, H. (2014) Microbial and animal rhodopsins: structures, functions, and molecular mechanisms. *Chem. Rev.* **114**, 126-163
3. Grote, M., and O'Malley, M. A. (2011) Enlightening the life sciences: the history of halobacterial and microbial rhodopsin research. *FEMS Microbiol. Rev.* **35**, 1082-1099
4. Bieszke, J. A., Braun, E. L., Bean, L. E., Kang, S., Natvig, D. O., and Borkovich, K. A. (1999) The *nop-1* gene of *Neurospora crassa* encodes a seven transmembrane helix retinal-binding protein homologous to archaeal rhodopsins. *Proc. Natl. Acad. Sci. U.S.A.* **96**, 8034
5. Spudich, J. L., and Jung, K.-H. (2005) Microbial rhodopsin: Phylogenetic and functional diversity. in *Handbook of photosensory receptors* (Briggs, W. R., and Spudich, J. L. eds.), Wiley-VCH Verlag, Weinheim. pp 1-23
6. Inoue, K., Kato, Y., and Kandori, H. (2014) Light-driven ion-translocating rhodopsins in marine bacteria. *Trends. Microbiol.* **23**, 91-98
7. Oesterhelt, D., and Stoeckenius, W. (1971) Rhodopsin-like protein from the purple membrane of *Halobacterium halobium*. *Nature* **233**, 149-152
8. Matsuno-Yagi, A., and Mukohata, Y. (1977) Two possible roles of bacteriorhodopsin; a comparative study of strains of *Halobacterium halobium* differing in pigmentation. *Biochem. Biophys. Res. Commun.* **78**, 237-243
9. Béjà, O., Aravind, L., Koonin, E. V., Suzuki, M. T., Hadd, A., Nguyen, L. P., Jovanovich, S. B., Gates, C. M., Feldman, R. A., Spudich, J. L., Spudich, E. N., and DeLong, E. F.

(2000) Bacterial Rhodopsin: Evidence for a New Type of Phototrophy in the Sea. *Science* **289**, 1902-1906

10. Béjà, O., Pinhassi, J., and Spudich, J. L. (2013) Proteorhodopsins: widespread microbial light-driven proton pumps. in *Encyclopedia of Biodiversity* (Levin, S. A. ed.), 2nd Ed., Elsevier, New York. pp 280-285

11. Jung, K. H. (2012) New type of cation pumping microbial rhodopsins in marine bacteria. in *244th ACS National Meeting & Exposition*, Philadelphia, PA

12. Yoshizawa, S., Kumagai, Y., Kim, H., Ogura, Y., Hayashi, T., Iwasaki, W., DeLong, E. F., and Kogure, K. (2014) Functional characterization of flavobacteria rhodopsins reveals a unique class of light-driven chloride pump in bacteria. *Proc. Natl. Acad. Sci. U.S.A.* **111**, 6732-6737

13. Inoue, K., Ono, H., Abe-Yoshizumi, R., Yoshizawa, S., Ito, H., Kogure, K., and Kandori, H. (2013) A light-driven sodium ion pump in marine bacteria. *Nat. Commun.* **4**, 1678

14. Inoue, K., Koua, F. H., Kato, Y., Abe-Yoshizumi, R., and Kandori, H. (2014) Spectroscopic study of a light-driven chloride ion pump from marine bacteria. *J. Phys. Chem. B* **118**, 11190-11199

15. Sasaki, J., Brown, L. S., Chon, Y. S., Kandori, H., Maeda, A., Needleman, R., and Lanyi, J. K. (1995) Conversion of bacteriorhodopsin into a chloride ion pump. *Science* **269**, 73-75

16. Havelka, W. A., Henderson, R., and Oesterhelt, D. (1995) Three-dimensional structure of halorhodopsin at 7 A resolution. *J. Mol. Biol.* **247**, 726-738

17. Váró, G., Brown, L. S., Needleman, R., and Lanyi, J. K. (1996) Proton transport by halorhodopsin. *Biochemistry* **35**, 6604-6611

18. Muroda, K., Nakashima, K., Shibata, M., Demura, M., and Kandori, H. (2012) Protein-

bound water as the determinant of asymmetric functional conversion between light-driven proton and chloride pumps. *Biochemistry* **51**, 4677-4684

19. Saitou, N., and Nei, M. (1987) The neighbor-joining method: a new method for reconstructing phylogenetic trees. *Mol. Biol. Evol.* **4**, 406-425

20. Jones, D. T., Taylor, W. R., and Thornton, J. M. (1992) The rapid generation of mutation data matrices from protein sequences. *Comput. Appl. Biosci.* **8**, 275-282

21. Sato, M., Kikukawa, T., Araiso, T., Okita, H., Shimono, K., Kamo, N., Demura, M., and Nitta, K. (2003) Roles of Ser130 and Thr126 in chloride binding and photocycle of *pharaonis* halorhodopsin. *J. Biochem.* **134**, 151-158

22. Yamashita, Y., Kikukawa, T., Tsukamoto, T., Kamiya, M., Aizawa, T., Kawano, K., Miyauchi, S., Kamo, N., and Demura, M. (2011) Expression of *salinarum* halorhodopsin in *Escherichia coli* cells: solubilization in the presence of retinal yields the natural state. *Biochim. Biophys. Acta* **1808**, 2905-2912

23. Hernández-Mariné, M., Fernández, M., and Merino, V. (1992) *Mastigocladopsis repens* (Nostochopsaceae), a new cyanophyte from Spanish soils. *Cryptogamie, Algol.* **13**, 113-120

24. Shih, P. M., Wu, D., Latifi, A., Axen, S. D., Fewer, D. P., Talla, E., Calteau, A., Cai, F., Tandeau de Marsac, N., Rippka, R., Herdman, M., Sivonen, K., Coursin, T., Laurent, T., Goodwin, L., Nolan, M., Davenport, K. W., Han, C. S., Rubin, E. M., Eisen, J. A., Woyke, T., Gugger, M., and Kerfeld, C. A. (2013) Improving the coverage of the cyanobacterial phylum using diversity-driven genome sequencing. *Proc. Natl. Acad. Sci. U.S.A.* **110**, 1053-1058

25. Chandrababunaidu, M. M., Singh, D., Sen, D., Bhan, S., Das, S., Gupta, A., Adhikary, S. P., and Tripathy, S. (2015) Draft Genome Sequence of *Tolypothrix boutellei* Strain

VB521301. *Genome Announc.* **3**, e00001-15

26. Singh, D., Chandrababunaidu, M. M., Panda, A., Sen, D., Bhattacharyya, S., Adhikary, S. P., and Tripathy, S. (2015) Draft Genome Sequence of Cyanobacterium *Hassallia byssoidea* Strain VB512170, Isolated from Monuments in India. *Genome Announc.* **3**, e00064-15

27. Das, A., Panda, A., Singh, D., Chandrababunaidu, M. M., Mishra, G. P., Bhan, S., Adhikary, S. P., and Tripathy, S. (2015) Deciphering the Genome Sequences of the Hydrophobic Cyanobacterium *Scytonema tolypothrichoides* VB-61278. *Genome Announc.* **3**, e00228-15

28. Das, S., Singh, D., Madduluri, M., Chandrababunaidu, M. M., Gupta, A., Adhikary, S. P., and Tripathy, S. (2015) Draft Genome Sequence of Bioactive-Compound-Producing Cyanobacterium *Tolypothrix campylonemoides* Strain VB511288. *Genome Announc.* **3**, e00226-15

29. Stanier, R. Y., Kunisawa, R., Mandel, M., and Cohen-Bazire, G. (1971) Purification and properties of unicellular blue-green algae (order *Chroococcales*). *Bacteriol. Rev.* **35**, 171-205

30. Rippka, R., Deruelles, J., Waterbury, J. B., Herdman, M., and Stanier, R. Y. (1979) Generic assignments, strain histories and properties of pure cultures of cyanobacteria. *J. Gen. microbiol.* **111**, 1-61

31. Keshari, N., and Adhikary, S. P. (2013) Characterization of cyanobacteria isolated from biofilms on stone monuments at Santiniketan, India. *Biofouling* **29**, 525-536

32. Jung, K.-H., Trivedi, V. D., and Spudich, J. L. (2003) Demonstration of a sensory rhodopsin in eubacteria. *Mol. Microbiol.* **47**, 1513-1522

33. Schobert, B., and Lanyi, J. K. (1982) Halorhodopsin is a light-driven chloride pump. *J.*

Biol. Chem. **257**, 10306-10313

34. Váró, G., Brown, L. S., Sasaki, J., Kandori, H., Maeda, A., Needleman, R., and Lanyi, J. K. (1995) Light-driven chloride ion transport by halorhodopsin from *Natronobacterium pharaonis*. I. The photochemical cycle. *Biochemistry* **34**, 14490-14499

35. Scharf, B., and Engelhard, M. (1994) Blue halorhodopsin from *Natronobacterium pharaonis*: wavelength regulation by anions. *Biochemistry* **33**, 6387-6393

36. Váró, G., Zimányi, L., Fan, X., Sun, L., Needleman, R., and Lanyi, J. K. (1995) Photocycle of halorhodopsin from *Halobacterium salinarium*. *Biophys. J.* **68**, 2062-2072

37. Hasegawa, C., Kikukawa, T., Miyauchi, S., Seki, A., Sudo, Y., Kubo, M., Demura, M., and Kamo, N. (2007) Interaction of the halobacterial transducer to a halorhodopsin mutant engineered so as to bind the transducer: Cl^- circulation within the extracellular channel. *Photochem. Photobiol.* **83**, 293-302

38. Oesterhelt, D. (1995) Structure and function of halorhodopsin. *Isr. J. Chem.* **35**, 475-494

39. Avetisyan, A. V., Kaulen, A. D., Skulachev, V. P., and Feniouk, B. A. (1998) Photophosphorylation in alkalophilic halobacterial cells containing halorhodopsin: chloride-ion cycle? *Biochemistry (Moscow)* **63**, 625-628

40. Ihara, K., Narusawa, A., Maruyama, K., Takeguchi, M., and Kouyama, T. (2008) A halorhodopsin-overproducing mutant isolated from an extremely haloalkaliphilic archaeon *Natronomonas pharaonis*. *FEBS Lett.* **582**, 2931-2936

41. Falb, M., Pfeiffer, F., Palm, P., Rodewald, K., Hickmann, V., Tittor, J., and Oesterhelt, D. (2005) Living with two extremes: conclusions from the genome sequence of *Natronomonas pharaonis*. *Genome Res.* **15**, 1336-1343

42. Balashov, S. P. (2000) Protonation reactions and their coupling in bacteriorhodopsin. *Biochim. Biophys. Acta* **1460**, 75-94

43. Lanyi, J. K. (2004) Bacteriorhodopsin. *Annu. Rev. Physiol.* **66**, 665-688

44. Váró, G., Brown, L. S., Lakatos, M., and Lanyi, J. K. (2003) Characterization of the photochemical reaction cycle of proteorhodopsin. *Biophys. J.* **84**, 1202-1207

Part Ⅱ

Photochemical analysis of the light-driven chloride-pumping rhodopsin

Ⅱ-1 Abstract

Halorhodopsin from *Masigocladopsis repens* (MrHR) is a light-driven inward Cl^- pump and can be converted into an outward H^+ pump by a single amino acid replacement. It is anticipated that MrHR evolved from a H^+ pump but has not yet been highly optimized into a mature Cl^- pump. Thus, this protein is a good research subject for elucidating the optimization of the Cl^--pumping mechanism. Here, I performed a photochemical analysis of MrHR and its mutants. Comparison of the photocycle for transportable (Cl^-) and nontransportable (I^-) anions revealed that the Cl^- transfer from the extracellular side to the cytoplasmic side occurs during the L-to-N+O transition. Spectroscopic studies and H^+ transfer reaction measurement suggest that Asp-200 (Asp-212 in Bacteriorhodopsin) protonates in the unphotolyzed state and deprotonates during the L-to-N+O transition. The ion-transporting measurement indicates that the deprotonation of Asp-200 is essential to transport Cl^-. In contrast to this protonation in the dark state and deprotonation in the light state, other Cl^--pumping rhodopsins maintain the deprotonation of the corresponding aspartic acid in both the dark and light states. This difference indicates the result of the optimization for Cl- pumping.

Ⅱ-2 Introduction

Many microorganisms have photoactive proteins to utilize light for environmental information and as an energy source. Microbial rhodopsins form a photoactive protein family and consist of a bundle of seven transmembrane helices surrounding a chromophore, retinal, which binds to a conserved lysine residue in helix G via a protonated Schiff base (PSB)[1,2]. Upon light irradiation, photoisomerization of retinal from the all-*trans* to the 13-*cis* configuration triggers the cyclic photoreaction called the photocycle. During the photocycle, rhodopsin performs various roles, including light-driven ion-pumps[3,4], light-sensors[5,6], or light-gated ion-channels[7–9].

The originally discovered microbial rhodopsin is an outward proton (H^+) pump, bacteriorhodopsin[10] (BR), from *Halobacterium salinarum* and was found in 1971. The second rhodopsin, an inward chloride ion (Cl^-) pump, halorhodopsin[10] (HR), was found in *H. salinarum*. After 1999, advances in genome sequencing techniques led to the discovery of novel microbial rhodopsins in the genomes of various microorganisms [11–13]. The representatives are the outward H^+ pump from marine proteobacteria (PR)[14,15], the outward sodium (Na^+) pump from *Krokinobacter eikastus* (KR2)[16] and the Cl^- pump from *Nonlabens marinus* (NM-R3)[17] .

Ion pumps are abundant and widespread in various microorganisms for light energy utilization[3]. These pumps are mainly classified into the categories of outward H^+ and Na^+ pumps and an inward Cl^- pump. Despite their functional diversity, these ion pumps have essentially the same structural folding. Thus, they appear to share a common transport machinery, and their transportable ions are determined by essential residues at appropriate positions. Previous studies demonstrated the importance of three residues corresponding to Asp-85, Thr-89 and Asp-96 in BR for the determination of transportable

ions[3,18]. Asp-85 and Asp-96 play the roles of H^+ acceptor from PSB and H^+ donor to PSB, respectively. In the Na^+ pump, Thr-89 is replaced with Asp, which has a significant role in Na^+ pumping[16]. These three residues are designated the "motif"; these are DTD and DTE for BR and PR, NDQ for the Na^+ pump, TSA for archaeal HR and NTQ for NM-R3.

Recently, I characterized a novel cyanobacterial Cl^--pumping rhodopsin HR from the terrestrial cyanobacterium *Mastigocladopsis repens* and designated it MrHR[19]. MrHR has the TSD motif; the specific threonine and serine for Cl^--binding and aspartic acid for a H^+ donor: Thr-74, Ser-78 and Asp-85, respectively. Additionally, components of the complex that releases H^+ to the extracellular medium, Glu-194 and Glu-204 in BR (Glu-182 and Glu-192 in MrHR) are conserved in MrHR (Fig. 1). Thus, MrHR contains the characteristic residues of Cl^- and H^+ pumps. MrHR acts as a light-driven inward Cl^- pump. However, unlike other Cl^- pumps, MrHR could be converted to an outward proton pump by the replacement of a single amino acid. This result implies that MrHR evolved from a H^+ pump but is not a mature Cl^- pump. Thus, MrHR is good research subject for elucidating the relationship between the mechanisms of Cl^- pumps and H^+ pumps.

In this work, I performed a photochemical analysis of MrHR and its mutants. By comparing the photocycles of the Cl^--bound form (transportable) and the I^--bound form (nontransportable), I found that Cl^- transfer from the extracellular (EC) side to the cytoplasmic (CP) half channel occurs during the L-to-N+O transition. Interestingly, Asp-200, corresponding to the secondary counterion Asp-212 in BR, was probably protonated in the unphotolyzed state. Ion-pumping activity measurements showed that deprotonation of Asp-200 during the photocycle is important for the Cl^--transporting activity. Flash photolysis and proton transfer measurements indicate that deprotonation of Asp-200 is important for the L-to-N+O transition, at which Cl- moves from the EC side

to the CP half channel. On the basis of these results, we discuss the photocycle of cyanobacterial Cl^- pumps and its relationship to the H^+-pumping mechanism.

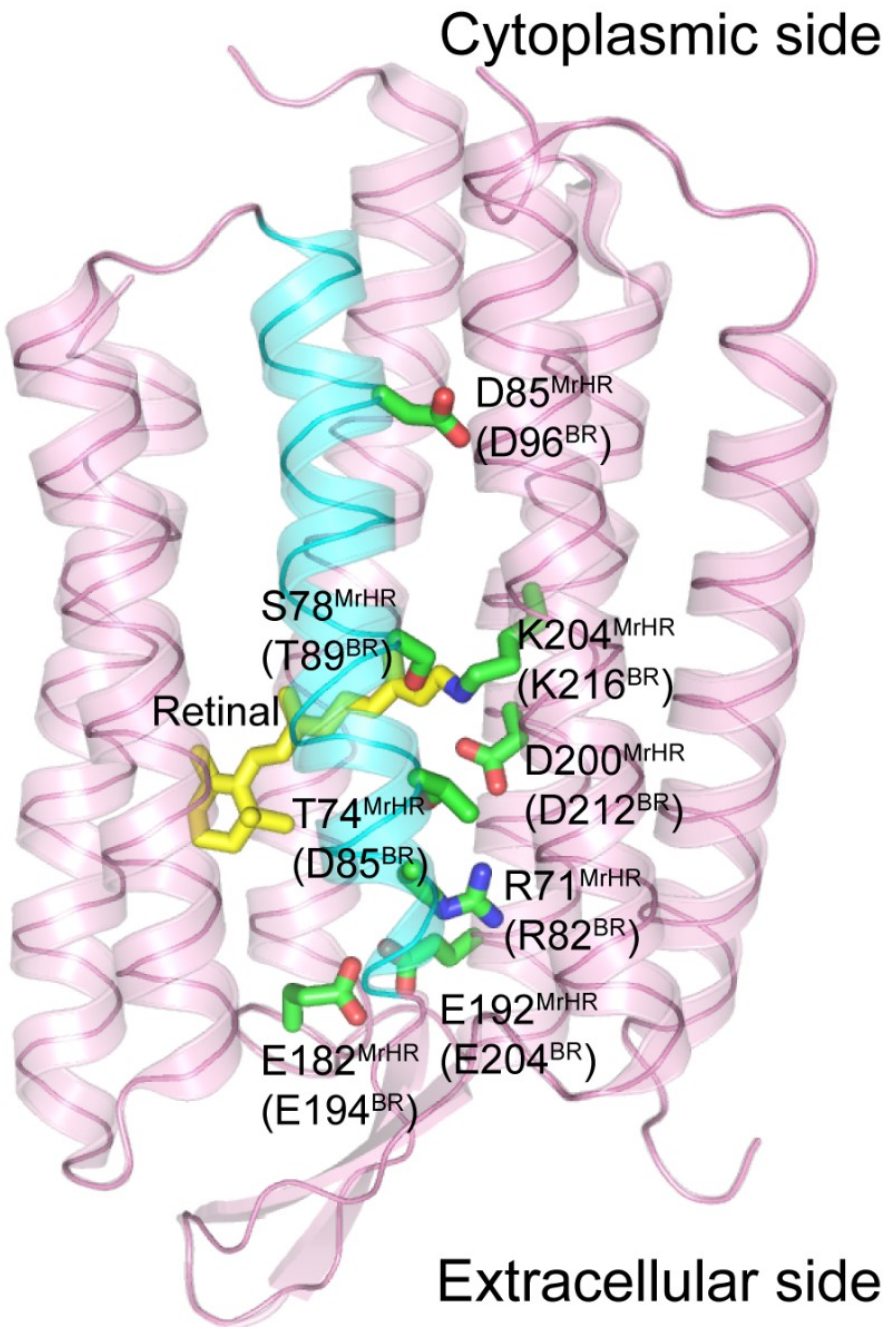

Figure 1. Position of important amino acid residues in MrHR. This figure is the X-ray crystal structure of BR (PDB code 1C3W) with modifications to indicate important residues of MrHR. This figure is shown from a view parallel to the membrane. Helix C is shown in cyan.

Ⅱ-3 Materials and Methods

Expression, purification and lipid reconstitution of MrHR

Escherichia coli strain DH5α was used for DNA manipulation. The construction of the expression plasmid of wild-type (WT) MrHR with additional amino acids in the C-terminus (-LEHHHHHH) was described previously[19]. The mutations were introduced using a site-directed mutagenesis kit (Strategene, La Jolla, CA). The correctness of mutant plasmids was confirmed by standard methods using an automated DNA sequencer (model 3100, Applied Biosystems, Foster City, CA). MrHR was expressed in and purified from *E. coli* strain BL21(DE3). The procedures were essentially same as those previously described[19,20]. In brief, the cells were grown in 2×YT medium at 37℃, and expression was induced by the addition of 1 mM isopropyl-ß-D-thiogalactopyranoside in the presence of 10 μM all-*trans* retinal. After 3 h of incubation, the colored cells were harvested by centrifugation and disrupted using a French press. The collected cell membrane fraction was solubilized with n-dodecyl ß-D-maltopyranoside (DDM) (Dojindo Lab, Kumamoto, Japan), and the solubilized MrHR was purified using nickel-nitrilotriacetic acid-agarose (Qiagen, Hilden, Germany). The purified samples were replaced with appropriate buffer solution by passage over Sephadex G-25 in a PD-10 column (Amersham Bioscience, Uppsala Sweden). For photo-induced proton transfer measurement, purified MrHR and its mutants were reconstituted into phosphatidylcholine (PC) liposomes at an MrHR:PC molar ratio of 1:30. The detergent was removed by gentle stirring overnight at 4℃ in the presence of SM2 Adsorbent Bio-Beads (Bio-Rad, Hercules, CA, USA). After filtration, the reconstituted MrHR was collected by centrifugation.

Spectroscopic measurements

Absorption spectra of unphotolyzed MrHR from 250-750 nm were measured using a UV1800 UV-Vis spectrometer (Shimadzu, Kyoto, Japan). All measurements were performed at room temperature. The samples contained a buffer component (MOPS, MES, or citric acid), 33 mM Na_2SO_4 and 0.1% DDM. The observed shifts in the absorption maxima were analyzed using the following Hill equation:

$$\Delta\lambda = \Delta\lambda_{\max} \frac{[Cl^-]^n}{{K_d}^n + [Cl^-]^n}$$

where $\Delta\lambda_{max}$ is the maximum shift of the wavelength, $[Cl^-]$ is the Cl^- concentration, K_d is the dissociation constant, and n is the Hill coefficient.

Flash photolysis measurements

The light-induced absorption changes in MrHR and its mutants were monitored by flash photolysis measurements. For the photoexcitation, the second harmonic (7 ns, 532 nm) of a Q-switched Nd:YAG laser was used The details were described previously[21]. To improve the S/N ratio, 30 laser pulses were used at each measurement wavelength. The temperature was maintained at 25℃ for all measurements. Data points on a logarithmic time scale were picked from the observed data for plots and the following analysis. The datasets, measured from 400-710 nm with a 10 nm interval, were analyzed using an irreversible sequential model: $P_0 \rightarrow P_1 \rightarrow P_2 \rightarrow \ldots \rightarrow P_i \rightarrow P_0$, where P_0 represents the original unphotolyzed state, and P_i represents the *i*th photochemically defined state[22]. This model contains only forward reactions between P_i states. Thus, these P_i states may contain a few physically defined intermediates when the reverse reactions exist between them. The details of the procedure were described previously[23]. Briefly, the data were fitted by a multi-exponential function simultaneously for a dataset of all wavelengths. The

appropriate number of exponents (*i*) was determined from the reduction in the standard deviation of the weight residues. The data weight was determined independently for each wavelength by estimating the average error from the baseline before laser irradiation (-44 to 0 ms). Using fitting results, the time constants τ_i and the absorption differences between P_i and P_0 ($\Delta\varepsilon_i$) were calculated. Independently, a P_0 spectrum was obtained by subtracting the background scattering ($A + B/\lambda^4$; λ in nm) from the measured spectrum of the unphotolyzed state in 4 M NaCl. Finally, absolute spectra of the P_i states were obtained by the adding the spectrum of P_0 to the absorption differences, $\Delta\varepsilon i$. For details of the analysis, refer to the paper by Chizhov[22] and our previous studies[23,24].

Chloride ion pump activity measurement

The ion-pumping activities of MrHR were measured in *E. coli* suspension using a conventional pH electrode method[25] that detected light-induced alkalization by passive H^+ transfer in response to the membrane potential created by the pump activity for chloride ions. The experimental details were described previously[19] Briefly, cells expressing MrHR were harvested at 3600 × g for 5 min at 4°C and washed twice with a 200 mM NaCl solution. They were resuspended in a 200 mM NaCl solution in the presence of 10 µM carbonyl cyanide m-chlorophenylhydrazone (CCCP) and gently shaken overnight. The samples were washed twice with 200 mM NaCl solution and finally suspended at an A660 of 0.5. The sample volume was 2.0 mL. Before measurements, 10 µM CCCP was added to the sample cuvette. For the activation of MrHR, 530±17.5 nm light from a green LED (LXHL-LM5C, Philips Lumileds Lighting Co., San Jose, CA) was used. After each measurement, the pH changes were converted to the molar amount of transported H^+ induced by the addition of known amounts of HCl.

Measurements of photo-induced proton transfer using an ITO transparent electrode

The flash-induced H^+ transfer was measured using an indium tin oxide (ITO) electrode, which acts as a time-resolved pH sensor[26–28]. In this experiment, PC-reconstituted MrHR was used. The reconstituted sample was suspended in distilled water at a protein concentration of ~10 μM. The suspension of approximately 100 μL was applied to the surface of the ITO electrode and then water was evaporated under reduced pressure to produce a dried film. Then, the unbound proteins were removed from the surface by washing with distilled water. This electrode was placed into an electrochemical cell, in which a buffer solution was sandwiched between two ITO electrodes: the ITO electrode that adsorbed the protein and a bare ITO for the reference electrode. The buffer solution contained the 6-mix buffer (citric acid/MES/MOPS/HEPES/CAPS/CHES) plus electrolyte (NaCl or NaI), and the pH was adjusted to the desired value (pH 5.0 - 6.5). The buffer capacity of this 6-mix buffer was constant over the entire examined pH range. The samples were excited by a 7 ns laser pulse (532 nm, 0.6 mJ/pulse) from a Q-switched Nd:YAG laser (Minilite I, Continuum, San Jose, CA, USA). The electrical signal from the ITO electrode was recorded after amplification by a homemade amplifier equipped with a 0.033 Hz low cut filter to remove fluctuations of baseline. To improve the S/N ratio, 60 laser pulses were used. The details were reported previously[27]

Ⅱ-4 Results

Cl^--transporting photocycle of wild-type MrHR

In previous works, I reported that MrHR can bind I^- but cannot transport it[19]. This result indicates that I^- cannot transfer from the vicinity of PSB to the CP half channel. It is anticipated that the photocycle of the I^--bound form lacks the intermediate necessary for the anion movement from the vicinity of PSB to the CP side and the following intermediates. To determine this intermediate, we compared the photocycles of Cl^--bound and I^--bound forms.

In 1.0 M NaCl (Fig. 2A), the photocycle is similar to that in 0.1 M NaCl. Previously, we described the photoreactions as follows[19]: MrHR→K→L→N+O→MrHR'→MrHR. K, MrHR', and the recovery of the ground state were monitored at 540 nm. L and N were monitored at 460 nm. O was monitored at 620 nm. Figure 2 A-D shows the photoreaction in 1.0 M NaCl. The main events of the photocycle were divided into three time ranges. From 10 μs to 0.16 ms (Fig. 2B), the transient absorption spectra with an isosbestic point show that the K-to-L transition is a simple reaction. Next, the transient absorption spectra from 0.16 ms to 4.5 ms show a broad absorption increase at 500-650 nm, suggesting the simultaneous formation of more than two distinguishable intermediates in this time range. I called the two intermediates N and O. After 4.5 ms, the two positive bands due to N and O decreased, and a single negative band at 540 nm increased. This band indicates the formation of MrHR'. The decay of MrHR' is very slow.

As I expected, the photocycle of the I^--bound form was clearly different from that of the Cl^--bound form (Fig. 2E). From 10 μs to 40 μs, the transient spectra were complicated due to retardation of the K-to-L transition (Fig. 2F, light gray lines). From 80 μs to 1.17 ms, a decrease in the absorbance at 540 nm was synchronized with an increase in the

absorbance at 460 nm (Fig. 2F solid lines). This transient absorption change is due to the decay of K and the formation of L, similarly to the photocycle of the Cl^--bound form. Different from the photocycle of the Cl^--bound form, a decrease in the absorbance at 460 nm was accompanied by an increase in the absorbance at 540 nm (Fig. 2G). Along with the transient absorption change, this result indicates an L-to-MrHR' transition. Thus, the photocycle of the I^--bound form lacks the N+O state, which suggests the L-to-N+O transition reflects the Cl^- transfer from the vicinity of PSB to the CP half channel.

For further insight into the photocycle of the Cl^--bound form, I performed global fitting analysis of the flash-induced absorbance changes. All datasets in 0.1 - 4.0 M NaCl were fitted by a sum of five exponential terms. These results indicate the existence of five photochemically defined states. The calculated spectra are shown in Fig. 3A. The spectra in 1.0 M NaCl with the putative components are shown in Fig. S1. Using an irreversible model, I calculated the spectra of the P_i state. In this model, the photocycle can be represented by several irreversible, kinetically defined P_i states. P_i contains a few physically defined intermediates. The P_1 state contains the L intermediate at approximately 500 nm and the long-wavelength intermediate (λmax > 560 nm), which corresponded to the state that was K designated in the previous work. The P_2 state contains only the L intermediate. P_3 and P_4 may contain two or three intermediates. The putative intermediates (N, O, and MrHR') in 1.0 M NaCl are indicated with gray dashed lines. P_5 presents MrHR', whose spectrum is almost same as that of the unphotolyzed state. It was difficult to determine the step relating to Cl^- release and reuptake due to lack of spectral alterations in response to a Cl^- concentration change. The time constants were also not affected by the Cl^- concentration (Fig. 3B).

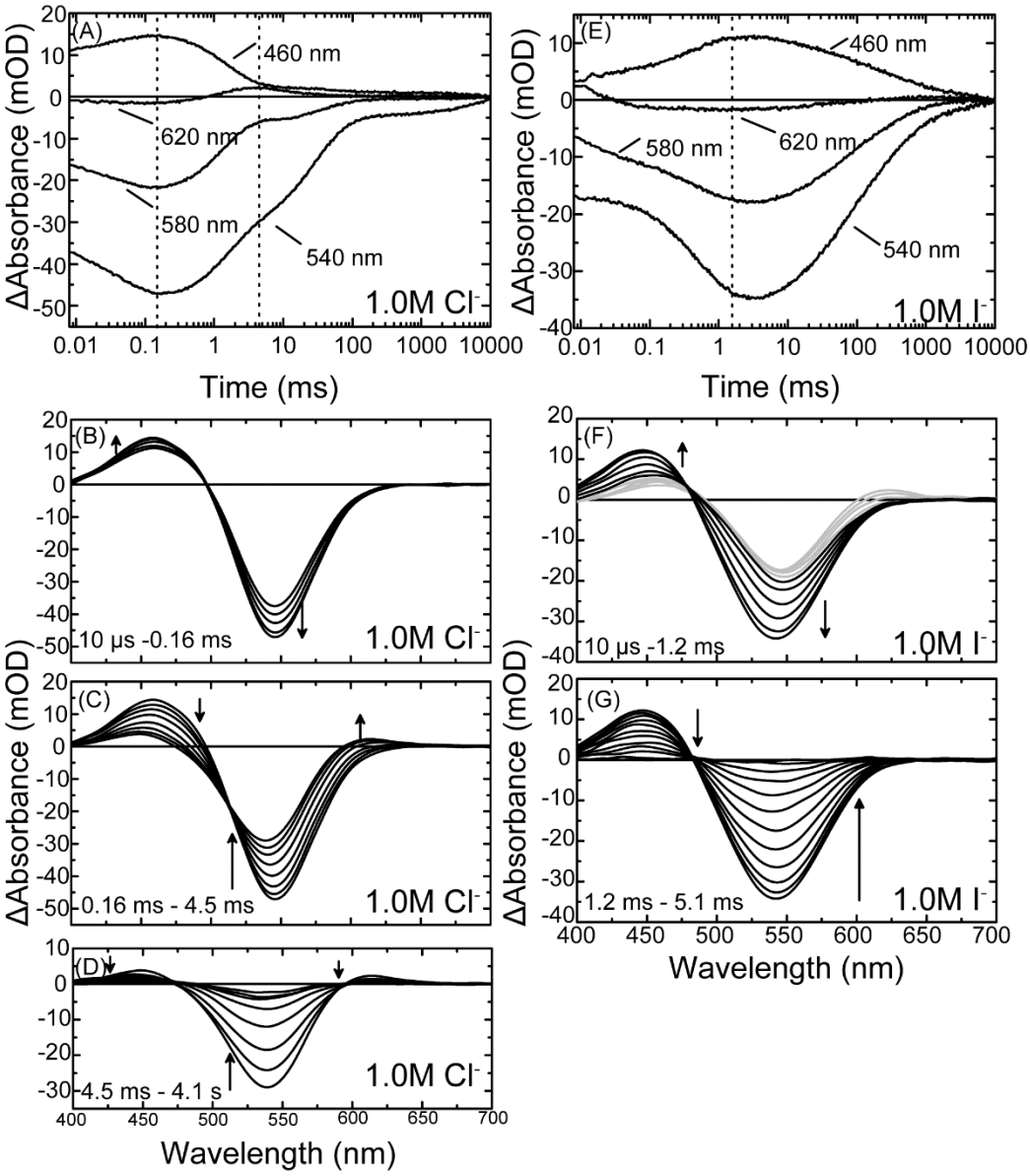

Figure 2. Comparison of MrHR photocycles for the Cl^--bound and I^--bound forms. The medium contains 1.0 M NaCl (A-D) or NaI (E-G), 10 mM MOPS (pH 6.5) and 0.1% DDM (w/V). Panels A and E show the results of flash-induced absorbance change at selected wavelengths. Panels B, C, D, F and G show the results of a series of flash-induced difference spectra in NaCl (B-D) and NaI (F and G). For the NaI results, difference spectra at 10-40 μs (panel F) are shown in gray lines.

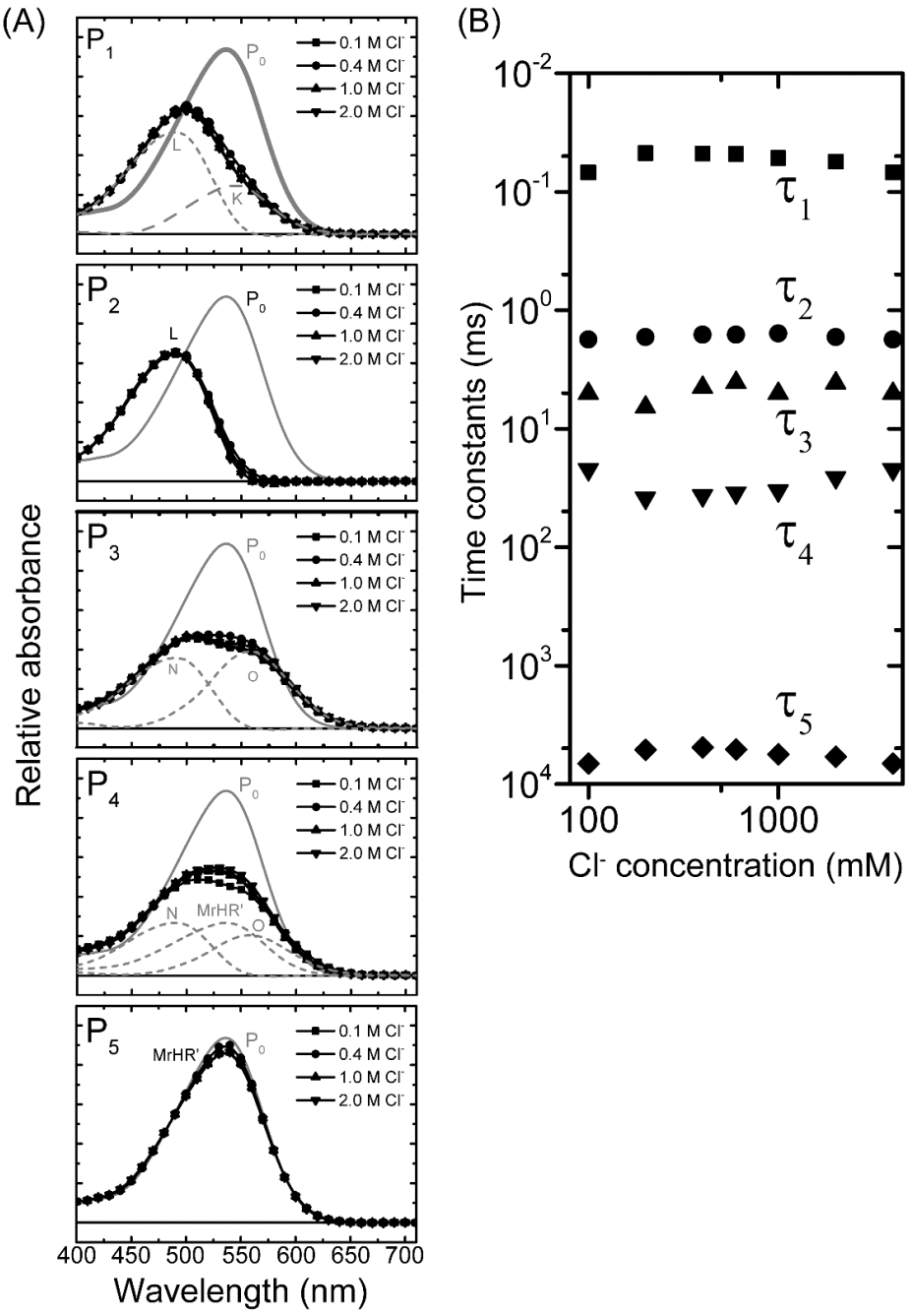

Figure 3. Results of global fitting of the flash photolysis data for wild-type MrHR at various NaCl concentrations. (A) Calculated absorption spectra of the kinetically defined states P_1-P_5 (black solid line) and the unphotolyzed state P_0 (gray solid line) The symbols show the concentration of NaCl (■: 0.1 M, ●: 0.4 M, ▲: 1.0 M, and ▼: 2.0 M). The broken gray lines show the predicted spectra of the components. (B) Cl^- concentration dependency of time constants (■: τ1, ●: τ2, ▲: τ3, ▼: τ4, and ◆: τ5).

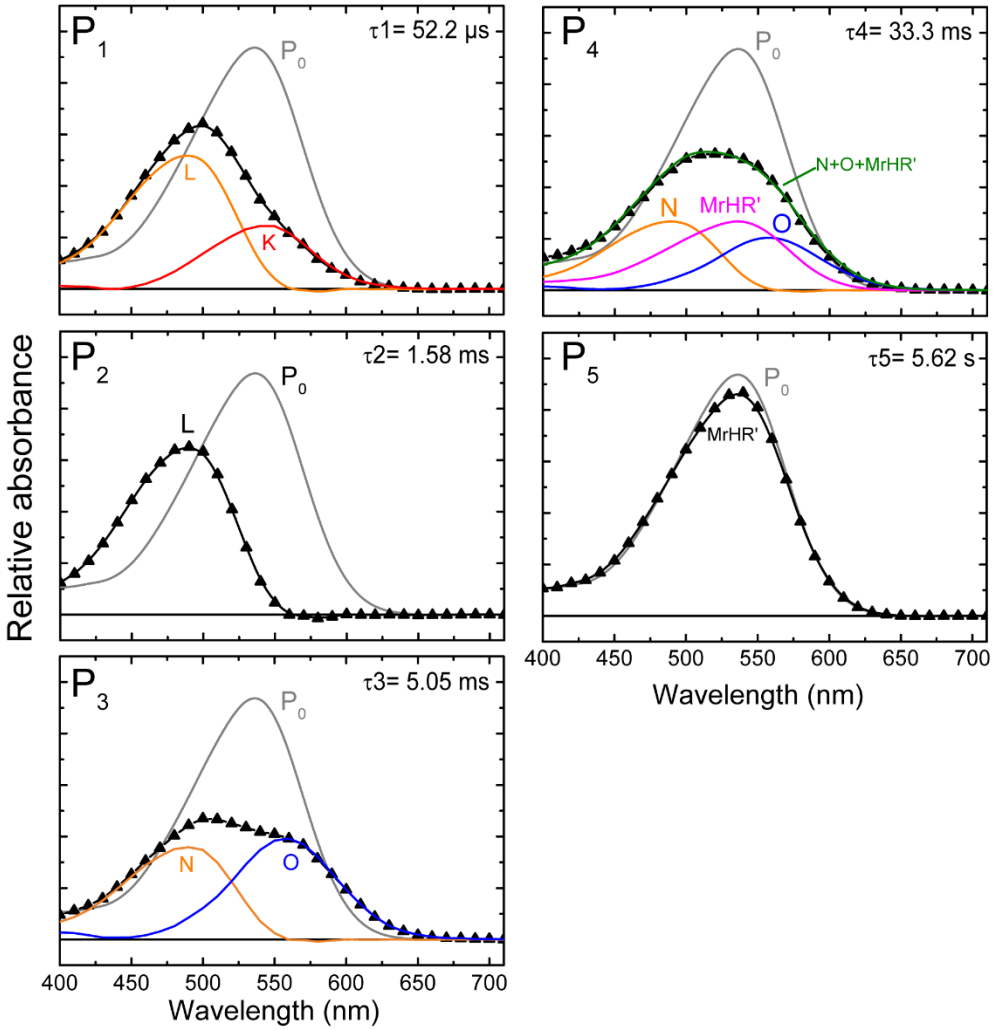

Figure S1. Results of global fitting of the flash photolysis data of wild-type MrHR in 1 M NaCl, including the spectra of the predicted components. Calculated absorption spectra of the kinetically defined states P_1-P_5 (black solid lines) and the unphotolyzed state P_0 (gray solid line). The colored lines show the spectra of the predicted components.

Chloride binding affinity and transporting activity of MrHR

I examined the Cl^- binding affinity of MrHR mutants. Cl^- pumps cause a spectral shift by binding Cl^- near the PSB. All mutants showed spectral shifts in response to the addition of Cl^-, suggesting that all mutants capture Cl^- near the PSB (Fig. 4A-H). In HsHR and NpHR, when the conserved arginine residue corresponding to Arg-71 in MrHR was replaced with Gln, these mutants lost the ability to bind Cl^- near the PSB. Thus, the role of this arginine in MrHR may be different from that of other Cl^- pumps. Unlike other Cl^- pumps except for HsHR, WT-MrHR showed a large red-shift. A spectral blue-shift was observed for T74A and E182Q (Fig. 4C and F). This result suggests that these residues are involved in spectral tuning. The dissociation constants (Kd) were determined from the relative λmax shift (Fig. 4I and Table 1). These results indicate that Arg-71, Thr-74, Ser78 and Glu-182 are important for binding Cl^- near the PSB. The corresponding residues of NpHR also contribute to the formation of the Cl^--binding site in the vicinity of PSB[24,29–31] (The spectra of NpHR-E234Q are unpublished data). D200 in MrHR corresponds D212 in BR, which remains deprotonated in the unphotolyzed state (pKa ~1). The absorption maxima of the BR-D212N mutant shifted by 9 nm from that of WT-BR[32] . In contrast, the absorption maxima of MrHR-D200N for the Cl^--bound and Cl^--free forms are almost the same as that of WT-MrHR (Fig. 4A and H). This result suggests the possibility that protonation of Asp-200 in WT-MrHR occurs in the unphotolyzed state.

Next, I examined the Cl^--transporting activities of MrHR mutants. We obtained colored cells expressing each MrHR mutant. After light irradiation, the medium was alkalized due to the passive proton influx in response to the light-driven inward Cl^--transport (Fig. 5A). The signals for R71Q, T74A and S78T were detected despite the

weak affinity of Cl^--binding (Fig. 5B-D). Substitution of the conserved H^+ donor and the residues forming the H^+-releasing complex also led to Cl^--transporting activity (Fig. 5F-G). However, only D200N did not cause the light-induced pH change. These results imply that protonation and/or deprotonation of Asp-200 is involved in the Cl^--transporting mechanism.

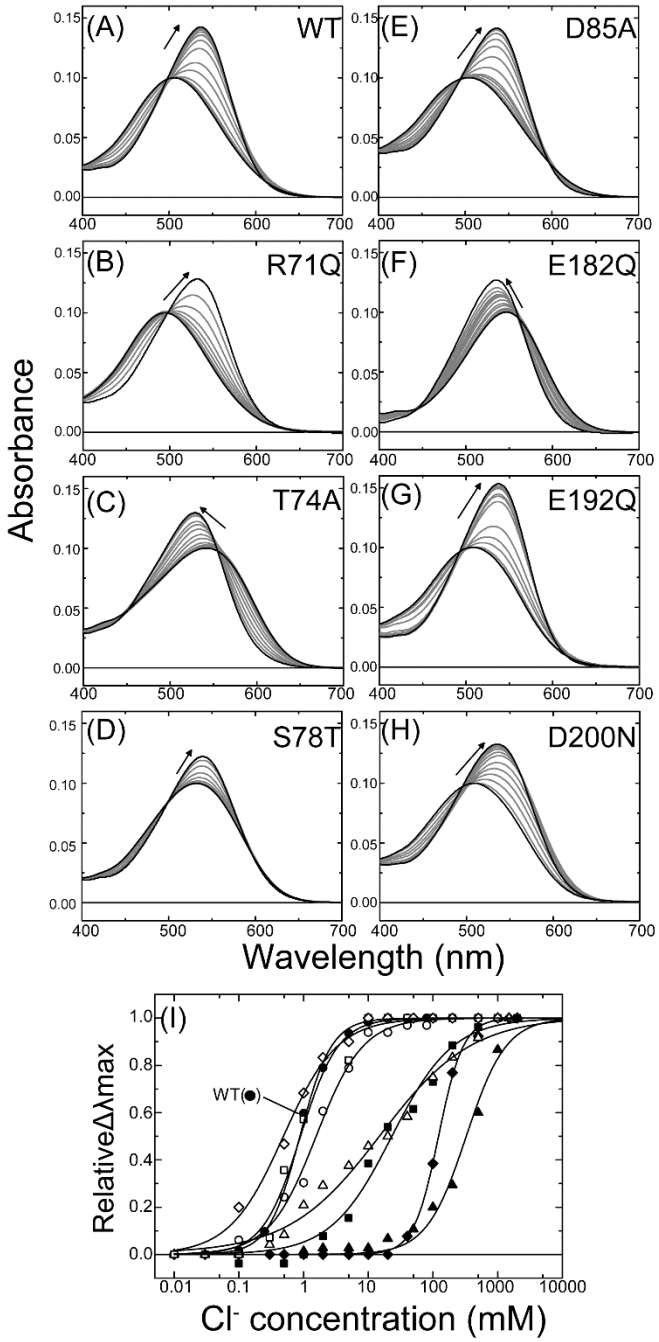

Figure 4. Cl^--induced spectral shift of MrHR.

The spectral change of WT-MrHR (A) and mutants (B-H). The medium (pH 5.0-6.5) contained 33 mM Na_2SO_4, 0.1% DDM and NaCl (0-0.5 or 2.0 M NaCl). Black arrows show the direction of the spectral shift induced by the addition of NaCl. (I) The relative λmax shifts are plotted. The symbols are as follows: ●: WT, ▲: R71Q, ■: T74A, ◆: S78T, ○: D85A, △: E182Q, □: E192Q, and ◇: D200N.

Table 1. Dissociation constants (K_d), Hill coefficients and absorption maxima (λ_{max}) of the Cl^--free and Cl^--bound forms and the shifts induced by chloride binding.

	K_d	Hill coefficient	Λmax ($-Cl^-$)	Λmax ($+Cl^-$)	Δλmax
	mM		*nm*	*nm*	*nm*
Wild-type	0.88 ± 0.02	1.78 ± 0.07	506	537	+31
R71Q	327 ± 24	1.41 ± 0.13	495	532	+37
T74A	23.1 ± 2.6	0.93 ± 0.08	542	529	-13
S78T	122 ± 1.95	2.27 ± 0.08	533	539	+6
D85A	1.56 ± 0.09	1.20 ± 0.08	506	536	+30
E182Q	15.3 ± 1.80	0.62 ± 0.04	547	535	-12
E192Q	0.90 ± 0.08	1.49 ± 0.20	509	537	+28
D200N	0.49 ± 0.03	1.04 ± 0.06	507	537	+30

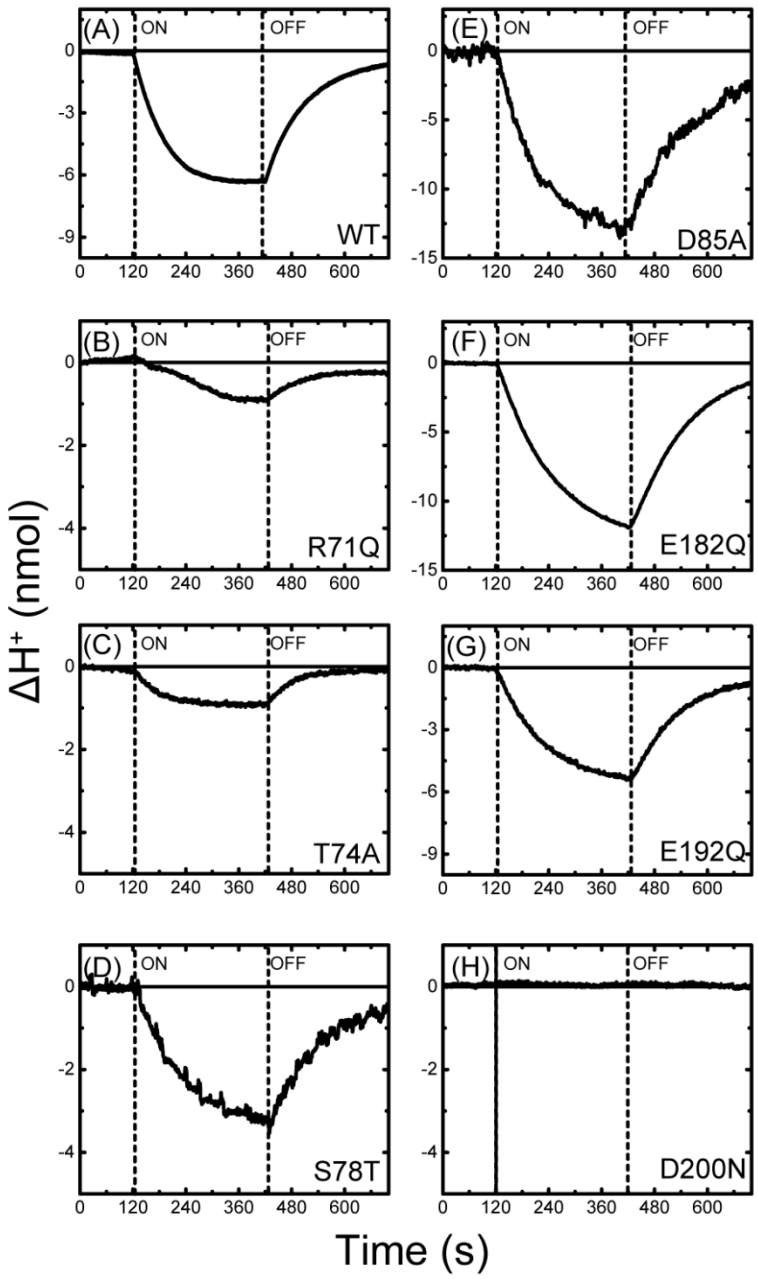

Figure 5. Light-induced chloride pumping activities by MrHR expressed *E. coli* cells: (A) WT, (B) R71Q, (C) T74A, (D) S78T, (E) D85A, (F) E182Q, (G) E192Q, and (H) D200N. Broken vertical lines show the beginning and end of light illumination. *E. coli* cells were suspended in 200 mM sodium chloride solution with 10 μM CCCP.

Photo-induced absorbance changes and H^+ transfer reactions of MrHR

Proton transfer reactions are related to the photocycles of not only proton pumps[33] but also sodium pumps[16,34] and photo-sensors[35]. Thus, we also measured the proton transfer reaction using an ITO electrode, which acts as highly time-resolved pH electrode[26–28]. In the Cl^--bound form of WT-MrHR, the H^+ release occurred at the L decay, and H^+ uptake followed (Fig. 6A). In contrast, for the I^--bound form of MrHR, the H^+ transfer signal did not increase (Fig. 6B). These results imply that H^+ transfer probably involves the anion transporting cycle.

To reveal the role of important residues during the photocycle, I examined the light-induced absorbance changes and H^+ transfer reactions of MrHR mutants. MrHR-R71Q underwent the same photocycle as WT-MrHR (Fig. 6B), unlike NpHR and the HsHR mutant whose arginine corresponding to Arg-71 in MrHR was replaced with glutamate. The photocycles of the T74A S78T mutants were similar to that of WT-MrHR (Fig. 6C and D). Replacement of Asp85 with alanine retarded the decay of the N+O state in MrHR (Fig. 6E). Asp-85 is located in the CP half channel, where Cl^- release occurs during the photocycle. The N+O formation is also delayed in D85N mutants (data not shown). The photocycle of D200N for the Cl^--bound form (Fig. 6I) is similar to that of WT-MrHR for the I^--bound form because the decay of L is synchronized to the formation of MrHR'. At pH 6.5, MrHR-D200N formed an M-like intermediate that was monitored at 400 nm due to deprotonation of PSB during the photocycle (Fig. S2). The I^--bound form of MrHR did not form an M-like intermediate. Thus, the rise of the M-like intermediate of D200N at pH 6.5 may be due to the amino acid replacement. The result for D200N at pH 5.0 is comparable to the result for WT-MrHR because WT-MrHR at pH 5.0 undergoes a light-induced H^+ release, similar to that at pH 6.5. Different from the Cl^--bound form of the

WT and other mutants, D200N did not exhibit the H^+ transfer reaction at pH 5.0. This result implies that Asp-200 is protonated in the unphotolyzed state and releases H^+ to the medium during the L decay. The mechanism for the Cl^- transfer from EC to CP involving the deprotonation of a conserved secondary counterion had not been observed for other Cl^- pumps previously.

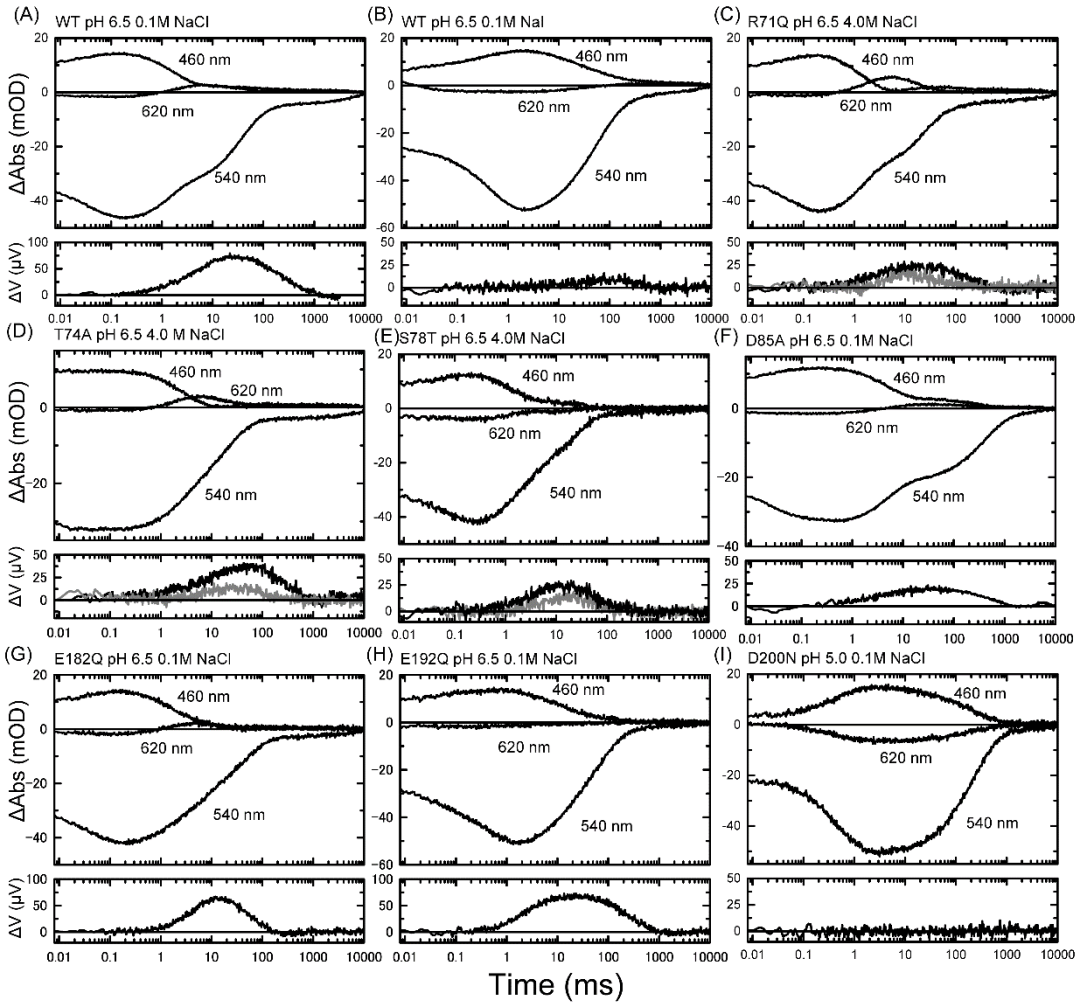

Figure 6. Comparisons between flash-induced absorbance changes (upper panels) at selected wavelengths and flash-induced H^+ transfer reactions (lower panels). For flash photolysis measurements, MrHR was solubilized in 0.1% DDM. Egg-PC reconstituted MrHR was used in H^+ transfer measurements. The medium was 0.1 M (black line) or 4.0 M (gray line) NaCl or 0.1 M NaI with the 6-mix buffer.

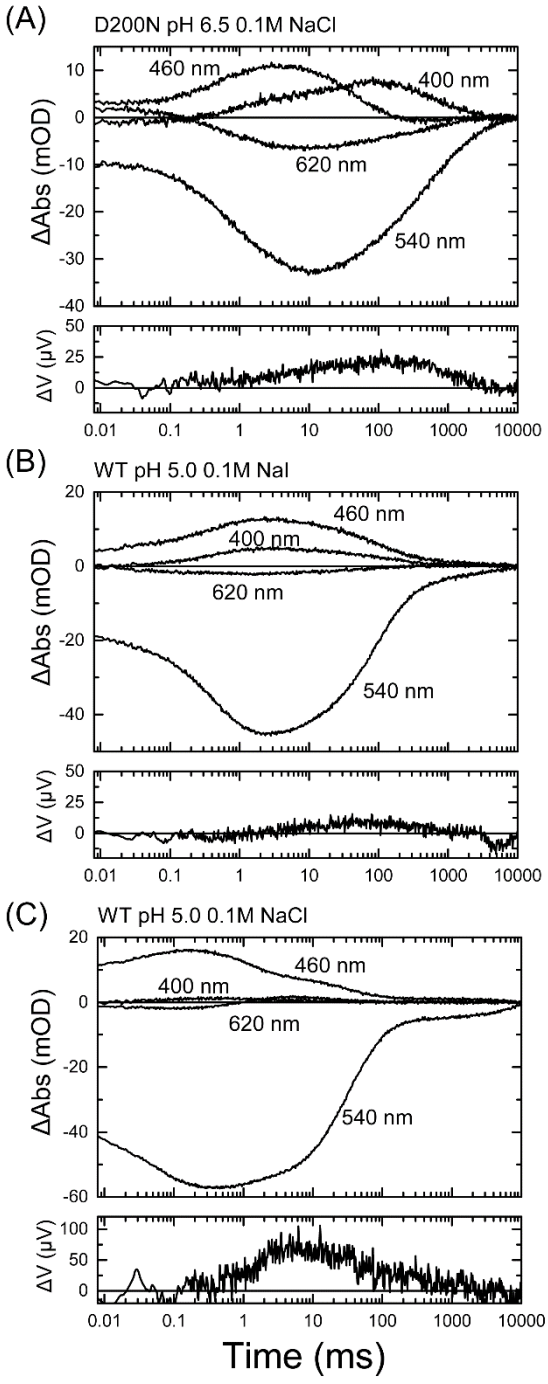

Fig. S2 Comparisons between flash-induced absorbance changes at selected wavelengths and flash-induced H^+ transfer reactions of (A) D200N at pH 6.5 in 0.1 M NaCl, (B) WT-MrHR at pH 6.5 in 0.1 M NaI and (C) WT-MRHR at pH 5.0 in 0.1 M NaCl. Upper panels show flash-induced absorbance changes at selected wavelengths. Lower panels show flash-induced H^+ transfer reactions. For flash photolysis measurements, MrHR solubilized in 0.1% DDM was used. Egg-PC reconstituted MrHR was used for H^+ transfer measurements.

Ⅱ-5 Discussion

Cl- translocation during the photocycle

Figure 7 shows the putative photocycle of MrHR. For MrHR, comparison of the photocycles of the Cl^--bound and I^--bound forms revealed that Cl^- transfer from the EC side to the CP side occurs during the L-to-N+O transition. In the unphotolyzed state, the spectra of the I^--bound form is almost the same as that of the Cl^--bound form[19]. Thus, the lack of N+O states results from a difference in the photocycles rather than the initial states. Different from that of NpHR, the photocycle of MrHR hardly changed in response to the addition of Cl-. By analogy to HsHR, the lack of an apparent change in the equilibrium state in response to changes in Cl^- concentration is presumably caused by kinetic reasons[36]. Therefore, it is difficult to determine the states relating to Cl^- release and uptake reactions. Another clue regarding the Cl^- transfer steps is the photocycle of the MrHR-D85A mutant. Asp-85 is located on the CP side that releases Cl^-. Retardation of the decay of N+O state indicates that a decay of N or O may be related to Cl^- release. However, the photocycle of D85A in 4.0 M NaCl is similar to that in 0.1 M NaCl (data not shown). These results suggest that the equilibrium state may reflect a factor other than the Cl^- binding (e.g., a local pH change and a conformational change).

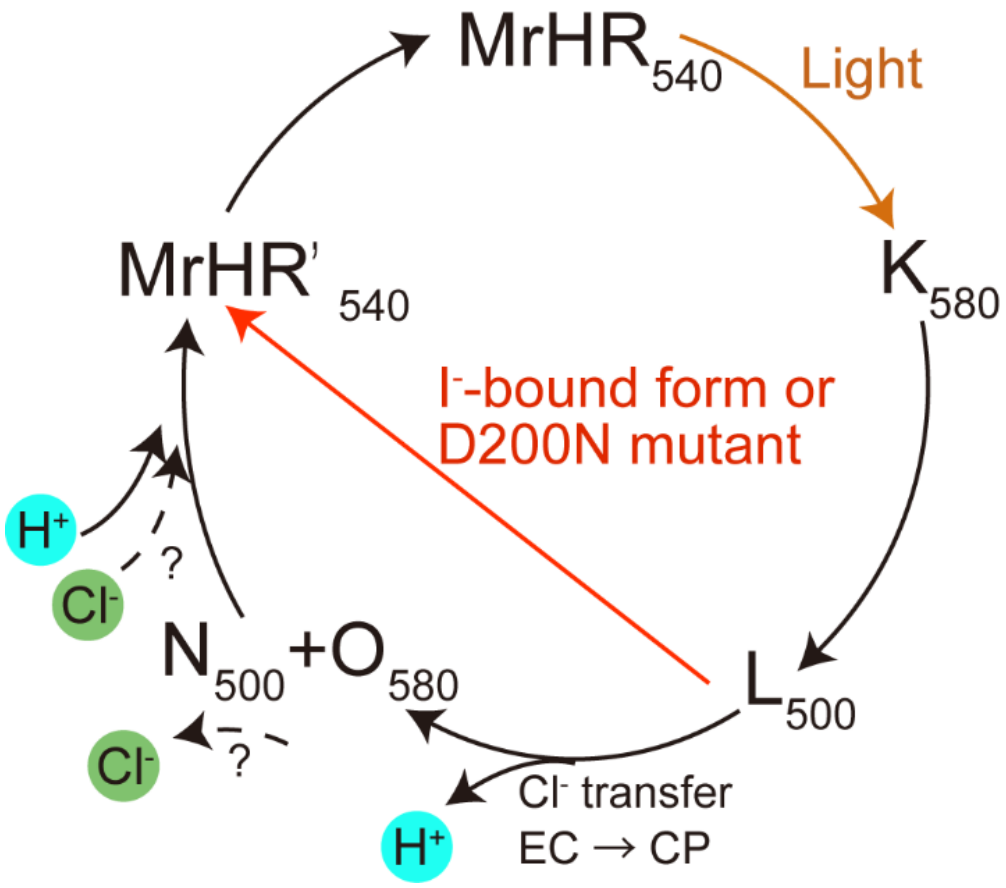

Figure 7. Putative photocycle model of MrHR. Dashed lines show the predicted Cl^- release and uptake sequences.

Role of the conserved residues, including the TSD motif

The important residues for Cl^- binding in MrHR are same as the corresponding residues in NpHR. However, the role of Arg-71 is different from that of the corresponding residue in NpHR and HsHR. In HsHR and NpHR[27], the Cl^- binding capability is lost in the Arg-to-Gln mutant. MrHR-R71Q captured Cl^- in the high NaCl concentration condition. This difference indicates that MrHR may have a mechanism for Cl^- binding without the conserved arginine residue.

My results suggest that Asp-200 becomes protonated in the unphotolyzed state at neutral pH. This is unusual behavior. In natural ion-pumping rhodopsins, the specific aspartic acid necessary for the secondary counterion to stabilize the electric quadrupole near the PSB is conserved. Thus, it is desirable to deprotonate the aspartic acid. In contrast to naturally occurring ion pumps, it was previously reported that Asp-212 of BR-D85T, which act as a Cl^- pump, has a pKa of 6.9 in the saturated NaCl solution. By analogy with the conversion of the BR-D85T and D85S mutants to Cl^- pumps, we provide two reasons for the high pKa of Asp-200. First, judging from the X-ray crystal structures, HsHR[37] and NpHR[38] contain three water molecules that can bind anions. These water molecules interact specifically with serine residues corresponding to Ser-73, Ser-78 and Ser-235 in HsHR. In contrast, BR-D85S[39] retains only one water molecule. BR-D85S and MrHR do not contain the serine residues. This difference affects the polar environment near the PSB. Second, the crystal structure of BR-D85S binding Br^- shows a direct interaction between Br^- and Asp-212, suggesting inhibition of the deprotonation of Asp-212 due to an electrostatic interaction. Asp-200 in MrHR may directly interact with anions. In analogy with Asp-212 in BR-D85T and D85S, the pKa of Asp-200 in MrHR in the unphotolyzed state increases.

Replacement of T74 and E182 affects the spectral tuning. One possible explanation is the deprotonation of Asp-200 in the unphotolyzed MrHR in the Cl^--free form for the T74A and E182Q mutants. The λmax without Cl^- for NpHR-D252N is shifted to a shorter wavelength than that of the Cl- bound WT-NpHR (unpublished results). This result indicates that protonation of a secondary counterion affects the direction of the spectral shift. Our result suggests protonation of Asp-200 in MrHR. The replacement of Thr-74 likely affects the pKa of Asp-200 in the Cl^--free state because Thr-74 is close to Asp-200 and PSB. Although Glu-182 is far from Asp-200 in MrHR, they may have a long-range interaction via internal water molecules and polar residues.

Except for the D200N mutant, all mutants underwent the photocycle and transported Cl^-. In T74A, the decay of the K intermediate was faster than that of WT-MrHR. This result may suggest that Cl^- movement occurred around Thr-74 during the K-to-L transition. MrHR-S78T had a photocycle similar to that of WT-MrHR. This result indicates that the contribution of Ser-78 in MrHR is less than that of Ser-130 in NpHR for the Cl^--transporting photocycles. However, we did not obtain the active form MrHR-mutants in which Ser-78 was replaced with Ala, Val, or Cys (data not shown). Thus, the O-H group at Ser-78 may be important for protein folding. As mentioned above, the decay of the N+O state is slow in the D85A mutant. This delay occurs also in the MrHR-D85N mutant, suggesting that deprotonation of Asp-85 may be important for the decay of the N+O state. The intensity of the H^+ transfer signal in D85A was weaker than that of WT-MrHR (Fig. 6F). Because D85A and D85N transported Cl^- similarly to WT, the deprotonation of Asp-85 does not seem to be required for Cl^- transport. The conserved Arg (Arg-71 in MrHR) is crucial for the photocycle of other ion pumps[16,29,31,40]. This arginine is conserved for Cl^- uptake in HRs. This uptake relates to the movement of

arginine. Conversely, MrHR-R71Q showed Cl^--transporting activity, suggesting that Arg-71 is not essential for the Cl^--transporting step of MrHR. This finding may mean that MrHR has an alternative mechanism for ion translocation that does not require the movement of this arginine.

Photo-induced proton release during the L-to-N+O transition

Upon light irradiation, the H^+ release reaction occurred in MrHR. The reaction was synchronized with the L decay, which reflects the Cl^- transfer from the EC side to the CP side. The candidates for H^+ release are four residues: Asp-85, Glu-182, Glu-192 and Asp-200. The following H^+ transfer reactions of Cl^- pumps have been reported. BR-D85T, which functions as a Cl^- pump, caused a photo-induced H^+-releasing reaction at Glu-204 during the formation of the O intermediate. In NpHR, deprotonation of the Glu-234 corresponding to Glu-182 in MrHR was detected by Fourier transform infrared spectroscopy (FTIR) [41]. Both H^+ releases are not necessary for Cl^- pumping. MrHR conserves the H^+ donor Asp-85. Conversely, as mentioned above, only replacement of Asp-200 with asparagine decreased the H^+ release signal. These results strongly suggest that Asp-200 acts as the H^+-releasing residue during the photocycle. I cannot exclude the possibility that protonated water acts as the proton source. Further studies using FTIR are needed to determine the direct proton source.

The role of the residues corresponding to D200 in MrHR is different from those of BR and HR. The photocycle of BR-D212N lacks the intermediates after L[32] in the neutral condition. Conversely, the photocycle of NpHR-D252N forms only a K intermediate (our unpublished results). D212 in BR contributes to the deprotonation of PSB during the L-to-M transition. The mechanism of the deprotonation of PSB is explained by a hydration

switch model[42]. In the hydration switch model, an internal water molecule connects to Asp-85 via a hydrogen bond in the ground, K and L intermediate states. The connection is conserved before the formation of M. Due to the rotation of the internal water molecule in the M intermediate, the internal water molecule loses the connection to Asp-85 and interacts with Asp-212 via a strong hydrogen bond. This switching cause an increase in the pKa of Asp-85, resulting in the capture of H^+ by Asp-85 during the formation of M. In this model, the pKa of Asp-212 decreases due to the strong hydrogen bond. We applied this model to the case of MrHR with a small modification. In the unphotolyzed state, the K and L intermediate states, Asp-200 does not connect to the internal water molecule. This supposition is consistent with the result that Asp-200 protonates in the unphotolyzed state. Asp-200 connects to the water via a strong hydrogen bond during the L-to-N+O transition, which induces the decrease in the pKa of Asp-200. As a result, Asp-200 releases H^+. Deprotonation of Asp-200 may trigger Cl^- transfer from the EC side to the CP half channel due to the electrostatic repulsion between two negative charges.

How sophisticated Cl^- pumps evolved from H^+ pumps

We revealed the relationship between H^+ release and Cl^- transfer in MrHR (Figure 7). Using these results and previous works, we can speculate about the process of optimization for a Cl^- pumping system from a H^+ pump. It is anticipated that the ancestral H^+ pump has the mechanism for transporting both H^+ and Cl^-. This hypothesis is supported by the previous report that BR can transport Cl^- below pH 0.55[43]. Replacement of the H^+ acceptor with neutral residues allows the original H^+ pump to gain Cl^--binding capabilities in the unphotolyzed state, such as in the BR-D85T and D85S mutants[44], and to lose the H^+-pumping activity. In contrast, this Cl^- pump shows

low affinity for Cl^- binding due to the lack of the conserved serine residue corresponding the Ser-78 in MrHR, which is important for the high affinity for Cl^- binding near the PSB. This immature Cl^- pump may undergo the essential H^+-releasing reaction for Cl^- pumping like MrHR. This reaction results from the protonation of a secondary counterion in the unphotolyzed state by the polar interaction surrounding the PSB and deprotonation of a secondary counterion during the photocycle by the hydration switch mechanism. After optimization for Cl^- pumping by molecular evolution, a mature Cl^- pump does not show this H^+ release due to the deprotonation of this Asp in the dark state. Thus, it is difficult to the convert a mature Cl^- pump to a H^+ pump by replacing several amino acids *in vitro*[45,46]

Ⅱ-6 Reference

(1) Ernst, O. P., Lodowski, D. T., Elstner, M., Hegemann, P., Brown, L. S., and Kandori, H. (2014) Microbial and animal rhodopsins: Structures, functions, and molecular mechanisms. *Chem. Rev.*

(2) Heberle, J., Deupi, X., and Schertler, G. (2014) Retinal proteins - You can teach an old dog new tricks. *Biochim. Biophys. Acta - Bioenerg. 1837*, 531–532.

(3) Inoue, K., Kato, Y., and Kandori, H. (2015) Light-driven ion-translocating rhodopsins in marine bacteria. *Trends Microbiol. 23*, 91–98.

(4) Oesterhelt, D., and Tittor, J. (1989) Two pumps, one principle: light-driven ion transport in halobacteria. *Trends Biochem. Sci. 14*, 57–61.

(5) Brown, L. S. (2014) Eubacterial rhodopsins - Unique photosensors and diverse ion pumps. *Biochim. Biophys. Acta - Bioenerg. 1837*, 553–561.

(6) Inoue, K., Tsukamoto, T., and Sudo, Y. (2014, June 1) Molecular and evolutionary aspects of microbial sensory rhodopsins. *Biochim. Biophys. Acta - Bioenerg.*

(7) Nagel, G., Szellas, T., Huhn, W., Kateriya, S., Adeishvili, N., Berthold, P., Ollig, D., Hegemann, P., and Bamberg, E. (2003) Channelrhodopsin-2, a directly light-gated cation-selective membrane channel. *Proc. Natl. Acad. Sci. U. S. A. 100*, 13940–5.

(8) Nagel, G., Ollig, D., Fuhrmann, M., Kateriya, S., Musti, A. M., Bamberg, E., and Hegemann, P. (2002) Channelrhodopsin-1: A Light-Gated Proton Channel in Green Algae. *Science (80-.). 296*, 2395–2398.

(9) Govorunova, E. G., Sineshchekov, O. A., Janz, R., Liu, X., and Spudich, J. L. (2015) Natural light-gated anion channels: A family of microbial rhodopsins for advanced optogenetics. *Science (80-.). 349*, 647–650.

(10) Oesterhelt, D., and Stoeckenius, W. (1971) Rhodopsin-like protein from the purple

membrane of Halobacterium halobium. *Nat. New Biol. 233*, 149–152.

(11) Bieszke, J. A., Braun, E. L., Bean, L. E., Kang, S., Natvig, D. O., and Borkovich, K. A. (1999) The nop-1 gene of Neurospora crassa encodes a seven transmembrane helix retinal-binding protein homologous to archaeal rhodopsins. *Proc Natl Acad Sci USA 96*, 8034–8039.

(12) Beja, O. (2000) Bacterial Rhodopsin: Evidence for a New Type of Phototrophy in the Sea. *Science (80-.). 289*, 1902–1906.

(13) Sharma, A. K., Spudich, J. L., and Doolittle, W. F. (2006) Microbial rhodopsins: functional versatility and genetic mobility. *Trends Microbiol. 14*, 463–469.

(14) Béjà, O., Spudich, E. N., Spudich, J. L., Leclerc, M., and DeLong, E. F. (2001) Proteorhodopsin phototrophy in the ocean. *Nature 411*, 786–789.

(15) Béjà, O., Aravind, L., Koonin, E. V, Suzuki, M. T., Hadd, a, Nguyen, L. P., Jovanovich, S. B., Gates, C. M., Feldman, R. a, Spudich, J. L., Spudich, E. N., and DeLong, E. F. (2000) Bacterial rhodopsin: evidence for a new type of phototrophy in the sea. *Science 289*, 1902–1906.

(16) Inoue, K., Ono, H., Abe-Yoshizumi, R., Yoshizawa, S., Ito, H., Kogure, K., and Kandori, H. (2013) A light-driven sodium ion pump in marine bacteria. *Nat. Commun. 4*, 1678.

(17) Inoue, K., Koua, F. H. M., Kato, Y., Abe-Yoshizumi, R., and Kandori, H. (2014) Spectroscopic study of a light-driven chloride ion pump from marine bacteria. *J. Phys. Chem. B 118*, 11190–11199.

(18) Inoue, K., Nomura, Y., and Kandori, H. (2016) Asymmetric functional conversion of eubacterial light-driven ion pumps. *J. Biol. Chem. 291*, 9883–9893.

(19) Hasemi, T., Kikukawa, T., Kamo, N., and Demura, M. (2016) Characterization of a cyanobacterial chloride-pumping rhodopsin and its conversion into a proton pump. *J. Biol. Chem. 291*, 355–362.

(20) Sato, M., Kikukawa, T., Araiso, T., Okita, H., Shimono, K., Kamo, N., Demura, M., and Nitta, K. (2003) Roles of ser130 and Thr126 in chloride binding and photocycle of pharaonis halorhodopsin. *J. Biochem. 134*, 151–158.

(21) Sato, M., Kikukawa, T., Araiso, T., Okita, H., Shimono, K., Kamo, N., Demura, M., and Nitta, K. (2003) Roles of ser130 and Thr126 in chloride binding and photocycle of pharaonis halorhodopsin. *J. Biochem. 134*, 151–158.

(22) Chizhov, I., and Engelhard, M. (2001) Temperature and Halide Dependence of the Photocycle of Halorhodopsin from Natronobacterium pharaonis. *Biophys. J. 81*, 1600–1612.

(23) Hasegawa, C., and Kikukawa, T. (2007) Interaction of the Halobacterial Transducer to a Halorhodopsin Mutant Engineered so as to Bind the Transducer: Cl− Circulation Within the Extracellular Channel†. *Photochem. ….*

(24) Sato, M., Kubo, M., Aizawa, T., Kamo, N., Kikukawa, T., Nitta, K., and Demura, M. (2005) Role of putative anion-binding sites in cytoplasmic and extracellular channels of Natronomonas pharaonis halorhodopsin. *Biochemistry 44*, 4775–4784.

(25) Yamashita, Y., Kikukawa, T., Tsukamoto, T., Kamiya, M., Aizawa, T., Kawano, K., Miyauchi, S., Kamo, N., and Demura, M. (2011) Expression of salinarum halorhodopsin in Escherichia coli cells: Solubilization in the presence of retinal yields the natural state. *Biochim. Biophys. Acta - Biomembr. 1808*, 2905–2912.

(26) Koyama, K., Miyasaka, T., Needleman, R., and Lanyi, J. K. (1998) Photoelectrochemical Verification of Proton-Releasing Groups in Bacteriorhodopsin. *Photochem. Photobiol. 68*, 400.

(27) Tamogami, J., Kikukawa, T., Miyauchi, S., Muneyuki, E., and Kamo, N. A tin oxide transparent electrode provides the means for rapid time-resolved pH measurements: application to photoinduced proton transfer of bacteriorhodopsin and proteorhodopsin.

Photochem. Photobiol. 85, 578–89.

(28) Reissig, L., Iwata, T., Kikukawa, T., Demura, M., Kamo, N., Kandori, H., and Sudo, Y. (2012) Influence of halide binding on the hydrogen bonding network in the active site of salinibacter sensory rhodopsin i. *Biochemistry 51*, 8802–8813.

(29) Kubo, M., Kikukawa, T., Miyauchi, S., Seki, A., Kamiya, M., Aizawa, T., Kawano, K., Kamo, N., and Demura, M. (2009) Role of Arg123 in light-driven anion pump mechanisms of pharaonis halorhodopsin. *Photochem. Photobiol. 85*, 547–555.

(30) Sato, M., Kikukawa, T., Araiso, T., Okita, H., Shimono, K., Kamo, N., Demura, M., and Nitta, K. (2003) Ser-130 of Natronobacterium pharaonis halorhodopsin is important for the chloride binding. *Biophys. Chem. 104*, 209–216.

(31) Rüdiger, M., and Oesterhelt, D. (1997) Specific arginine and threonine residues control anion binding and transport in the light-driven chloride pump halorhodopsin. *EMBO J. 16*, 3813–3821.

(32) Needlemant, R., Chang, M., Ni, B., Váró, G., Fornés, J., White, S. H., and Lanyi, J. K. (1991) Properties of Asp212 → Asn bacteriorhodopsin suggest that Asp212 and Asp85 both participate in a counterion and proton acceptor complex near the schiff base. *J. Biol. Chem. 266*, 11478–11484.

(33) Váró, G., Brown, L. S., Needleman, R., and Lanyi, J. K. (1996) Proton transport by halorhodopsin. *Biochemistry 35*, 6604–11.

(34) Kato, H. E., Inoue, K., Abe-Yoshizumi, R., Kato, Y., Ono, H., Konno, M., Hososhima, S., Ishizuka, T., Hoque, M. R., Kunitomo, H., Ito, J., Yoshizawa, S., Yamashita, K., Takemoto, M., Nishizawa, T., Taniguchi, R., Kogure, K., Maturana, A. D., Iino, Y., Yawo, H., Ishitani, R., Kandori, H., and Nureki, O. (2015) Structural basis for Na+ transport mechanism by a light-driven Na+ pump. *Nature 521*, 48–53.

(35) Spudich, E. N., Zhang, W., Alam, M., and Spudich, J. L. (1997) Constitutive signaling by the phototaxis receptor sensory rhodopsin II from disruption of its protonated Schiff base-Asp-73 interhelical salt bridge. *Proc. Natl. Acad. Sci. U. S. A. 94*, 4960–5.

(36) Váró, G., Zimányi, L., Fan, X., Sun, L., Needleman, R., and Lanyi, J. K. (1995) Photocycle of halorhodopsin from Halobacterium salinarium. *Biophys. J. 68*, 2062–2072.

(37) Kolbe, M., Besir, H., Essen, L. O., and Oesterhelt, D. (2000) Structure of the light-driven chloride pump halorhodopsin at 1.8 A resolution. *Science 288*, 1390–1396.

(38) Kouyama, T., Kanada, S., Takeguchi, Y., Narusawa, A., Murakami, M., and Ihara, K. (2010) Crystal structure of the light-driven chloride pump halorhodopsin from Natronomonas pharaonis. *J. Mol. Biol. 396*, 564–79.

(39) Facciotti, M. T., Cheung, V. S., Nguyen, D., Rouhani, S., and Glaeser, R. M. (2003) Crystal structure of the bromide-bound D85S mutant of bacteriorhodopsin: principles of ion pumping. *Biophys. J. 85*, 451–8.

(40) Balashov, S. P. (2000) Protonation reactions and their coupling in bacteriorhodopsin. *Biochim. Biophys. Acta - Bioenerg.*

(41) Shibata, M., Saito, Y., Demura, M., and Kandori, H. (2006) Deprotonation of Glu234 during the photocycle of Natronomonas pharaonis halorhodopsin. *Chem. Phys. Lett. 432*, 545–547.

(42) Kandori, H. (2004) Hydration switch model for the proton transfer in the Schiff base region of bacteriorhodopsin. *Biochim. Biophys. Acta - Bioenerg. 1658*, 72–79.

(43) Dér, A., Tóth-Boconádi, R., and Keszthelyi, L. (1989) Bacteriorhodopsin as a possible chloride pump. *FEBS Lett. 259*, 24–26.

(44) Sasaki, J., Brown, L. S., Chon, Y. S., Kandori, H., Maeda, a, Needleman, R., and Lanyi, J. K. (1995) Conversion of bacteriorhodopsin into a chloride ion pump. *Science 269*,

73–75.

(45) Havelka, W. A., Henderson, R., and Oesterhelt, D. (1995) Three-dimensional structure of halorhodopsin at 7 Å resolution. *J. Mol. Biol. 247*, 726–738.

(46) Muroda, K., Nakashima, K., Shibata, M., Demura, M., and Kandori, H. (2012) Protein-bound water as the determinant of asymmetric functional conversion between light-driven proton and chloride pumps. *Biochemistry 51*, 4677–84.

Concluding remarks

In this thesis, I performed functional analysis of a novel cyanobacterial rhodopsin, *Mastigocladopsis repens* halorhodopsin (MrHR). MrHR is a member of a novel cyanobacterial rhodopsin group and has the characteristic residues for Cl^- and H^+ pumps.

In part 1 of this thesis, I performed characterization of MrHR and its functional conversion. MrHR acts as a light-driven Cl^- pump. The transportable anions are severely restricted to only Cl^- and Br^-, different from the situation for HR and FR. The Cl^--transporting photocycle of MrHR is slower than that of other Cl^- pumps. Next, I attempted to convert MrHR to a H^+ pump; the mutant T74D was generated in which the Asp residue was introduced as a possible proton acceptor. MrHR was converted to an outward proton pump. The donor residue is not essential for the Cl^--pumping activity. However, in T74D, both the introduced acceptor and the conserved donor function are comparable to those in natural H^+ pumps. These results suggest that MrHR evolved from a H^+ pump, but the residues and the structure have not been optimized for a mature Cl^- pump.

In part 2 of this thesis, I performed a photochemical analysis of MrHR and its mutants to elucidate the process of the optimization for a Cl^- pumping system. The comparison of the photocycles for transportable (Cl^-) and nontransportable (I^-) anions revealed that Cl^- transfer from the extracellular side to the cytoplasmic side occurs during the L-to-N+O transition. However, the sequence of Cl^- release and uptake could not be determined due to the lack of an equilibrium state related to the Cl^- concentration. The Cl^--induced spectral changes showed that R71, T74, S78, and E182 are important for Cl^- binding in

the dark state. Spectroscopic studies and H^+ transfer reaction measurements suggest that Asp-200 protonates in the unphotolyzed state and deprotonates during the L-to-N+O transition. The results of ion-transporting measurements suggest that the deprotonation of Asp-200 is necessary for Cl^- transport. In contrast to this protonation in the dark state and deprotonation in the light state, other Cl^--pumping rhodopsins maintain the deprotonation of the corresponding aspartic acid in both the dark and light states. This difference indicates the result of the optimization for Cl- pumping.

In this thesis, I presented the functional characteristics of the novel chloride-pumping rhodopsin. I believe that my findings will be helpful for understanding the functional diversity of microbial rhodopsins and elucidating the mechanism for determining transportable ions.

Acknowledgements

I gratefully acknowledge invaluable suggestion and support of Professor Makoto Demura, Lecturer Takashi Kikukawa, Professor Naoki Kamo.

I would like to express my gratitude to Associate Professor Tomoyasu Aizawa, Assistant professor Masakatsu Kamiya.

I deeply appreciate Professor Masataka Kinjo for reviewing this paper.

I am grateful to Yumi Watanabe for her works.

I deeply thank my colleagues for many advice, discussion, and kindness in my daily life. Finally, I would like to express grateful appreciation to my family for many support and encouragement during my 9-years campus life in Hokkaido University